A mechanistically novel peptide agonist of the IL-7 receptor that addresses limitations of IL-7 cytokine therapy

A mechanistically novel peptide agonist of the IL-7 receptor

William J. Dower[1¶*], Angie Inkyung Park[1], Alice V. Bakker[1], Steven E. Cwirla[1], Praechompoo Pongtornpipat[1], Blake M. Williams[1,2], Prarthana Joshi[1], Bryan A. Baxter[1], Michael C. Needels[1], Ronald W. Barrett[1¶*]

[1]Medikine, Inc., Menlo Park, California, United States of America

[2] Department of Biomedical Engineering, and Center for Quantitative Bioinformatics and Quantitative Biology, Colleges of Engineering and Medicine, University of Illinois Chicago, IL, USA

¶ WD and RB are Joint Senior Authors

* Corresponding authors

E-mail: bdower@medikine.com (WD)

rbarrett@medikine.com (RB)

Abstract

Interleukin (IL)-7 is broadly active on T-cell populations, and modified versions have been clinically evaluated for a variety of therapeutic applications, including cancer, lymphopenia and infectious diseases; and found to be relatively well-tolerated and biologically active. Here we describe novel IL-7R agonists that are unrelated in structure to IL-7, bind to the receptor subunits differently from IL-7, but closely emulate IL-7 biology. The small size, low structural complexity, and the natural amino acid composition of the pharmacologically active peptide MDK1472 allows facile incorporation into protein structures, such as the IgG2-Fc fusion MDK-703. This molecule possesses properties potentially better suited to therapeutic applications than native IL-7 or its derivatives. We compared these compounds with IL-7 for immune cell selectivity, induction of IL-7R signaling, receptor-mediated internalization, proliferation, and generation of immune cell phenotypes in human and non-human primate (NHP) peripheral blood cells in vitro; and found them to be similar in biological activity to IL-7.

In cynomolgus macaques, MDK-703 exhibits a circulating half-life of 46 hr, and produces sustained T-cell expansion characteristic of IL-7 treatment. In the huCD34^{+}-engrafted NSG mouse model of the human immune system, MDK-703 induces an immune cell profile very similar to that generated by IL-7-derived compounds; including the pronounced expansion of memory T-cells, particularly the population of stem-like memory T-cells (Tscm), which may be important for anti-tumor activities reported with IL-7 treatment.

Clinical administration of IL-7 and modified variants has been reported to induce anti-drug antibodies (ADAs), including IL-7 neutralizing antibodies. The novel peptide agonist reported here scores very low in predicted immunogenicity, and because the peptide lacks

43 sequence similarity with IL-7, the problematic immunogenic neutralization of endogenous

44 cytokine should not occur.

45

Introduction

Interleukin-7 receptor (IL-7R) signaling is essential to establishing and sustaining immuno-competence throughout life. Most phases of T-cell development, and the continuing maintenance of T-cell homeostasis and functional responsiveness of the lymphoid system, depend on the availability of IL-7 and well-regulated control of its receptor expression. The absence of T-cells in patients with IL-7Rα mutations results in severe combined immune deficiency, revealing the essential role of the IL-7 system in healthy immune function [1, 2].

Unlike other cytokines regulating T-cell biology, IL-7 is produced primarily by non-hematopoietic tissues, among the most active of which is the stroma of lymphoid organs, including thymus and lymph nodes [3]. Upon secretion, most IL-7 is sequestered locally through binding to epithelia and ECM [4-6], and is detectable in the peripheral circulation of healthy humans at concentrations less than 10 pg/mL. Under normal conditions, T-cells experience limiting levels of IL-7 and must compete for this cytokine. While IL-7 levels are low and constant, IL-7Rα expression fluctuates, mediating cell selectivity and sensitivity [7]. Under conditions of T-lymphocyte depletion (lymphopenia caused by a variety of conditions such as viral infection, sepsis, cancer, and therapeutic interventions), the reduced number of T-cells internalize less IL-7, thereby elevating both local and circulating levels to provide proliferative stimulus and potential reversal of the lymphopenic condition [8].

The IL-7 receptor belongs to the family of interleukin receptors that share the common gamma subunit (γc). γc is ubiquitously expressed on immune cells, while private cytokine-specific α or β subunits are uniquely distributed among immune cell types, conferring the pattern of cell selectivity for each of the common gamma cytokines. Regulation of surface density of the

68 IL-7Rα subunit is a principal determinant of cell sensitivity to IL-7 stimulation; and IL-7
69 exposure modulates the surface density of IL-7Rα at two levels. First, upon IL-7 binding and
70 initiation of signaling, the activated receptor complexes are rapidly internalized, and IL-7Rα is
71 directed to late endosomes for degradation; second, IL-7R signaling down regulates transcription
72 of IL-7Rα. Besides the immediate effect on the cell surface level of IL-7Rα, internalization of
73 the signaling complex also depletes or "consumes" IL-7. The resulting decline in IL-7 and IL-7R
74 signaling relieves transcriptional suppression, allowing IL-7Rα expression and cell sensitivity to
75 IL-7 to rise. This fluctuation of IL-7 availability and IL-7Rα expression is intrinsic to the
76 feedback regulation of T-lymphocyte homeostasis. Recognition of this oscillating dynamic led to
77 the concept of IL-7 sharing (or competition) among T-cells that depend on the limited supply of
78 IL-7 for survival. This shared access to IL-7 seems key to maintaining healthy steady-state T-cell
79 populations - the immune homeostasis feature that characterizes IL-7 biology [9-11].
80 Among the cells most consistently responsive to IL-7 are naive and memory T-cells; both
81 are long-lived lymphocytes requiring periodic IL-7R stimulation. Throughout life, immuno-
82 competence depends on a naive T-cell population retaining proliferative and differentiation
83 potential, and IL-7 drives thymic generation, peripheral proliferation and survival, and T-cell
84 receptor (TCR) diversification to maintain a robust population of potential effectors. Following
85 immune response, IL-7 provides ongoing support of a select population of effectors that have
86 differentiated into memory cells [12].
87 Recently, IL-7R agonists have been shown to drive the generation of a "stem-like"
88 population of early memory/effector cells believed important for tumor suppression. IL-7
89 diversifies the TCR repertoire by inducing the expansion of less differentiated but more
90 proliferative T naïve (T_N) and stem cell-like memory T (T_{SCM}) subpopulations. T_{SCM} are a subset

91 of memory T-lymphocytes with the ability to rapidly self-renew and the capacity to reconstitute a
92 spectrum of memory and effector T-cell subsets. T_{SCM} may be necessary for the control of
93 persistent pathologies as antigen-driven effector cells undergo functional exhaustion and
94 replicative senescence, requiring continuous replenishment by less differentiated T-cell subsets
95 [13-15].

96 IL-7, through its influence on many lymphocyte classes, exerts broad influence on
97 immune readiness and response, and long-term memory capability, which suggests a variety of
98 immune-therapeutic applications for exogenous IL-7R agonists. This clinical potential is
99 supported by many animal studies evaluating effects of recombinant forms of IL-7 in models of
100 lymphopenia, infectious disease and sepsis, and cancer [11, 16-18]. In human studies,
101 recombinant IL-7 (non-glycosylated and glycosylated), and a pharmacokinetic (PK)-enhanced
102 Fc-fusion of IL-7 (efineptakin alfa) have been clinically evaluated for use in lymphopenia, septic
103 shock, infectious disease, enhancement of response to vaccination, lymphopenia associated with
104 COVID-19, autoimmune diseases, chronic inflammatory diseases, and cancer. These IL-7R
105 agonists appear to be relatively well-tolerated and biologically active in the clinic [16, 19-26].

106 Among the various indications, there is particularly strong interest in the use of IL-7R
107 agonists for treating cancer. Recombinant human (rh)IL-7 and modified forms, administered to
108 mice, NHP, and humans have been shown to induce widespread T-cell proliferation, increase T-
109 cell numbers, modulate peripheral T-cell subsets, and increase TCR repertoire diversity. In
110 oncology applications, these biological attributes, alone or in combination with other immune-
111 based therapies exhibit anti-tumor effects in mice and may enhance the rate, depth, and durability
112 of clinical responses. IL-7R agonists alone or in combination with checkpoint inhibitors have
113 been reported to increase the number and function of anti-tumor T lymphocytes in peripheral

114 blood of several cancer patient populations (e.g., checkpoint inhibitor [CPI]-naïve
115 relapsed/refractory microsatellite stable colorectal cancer [MSS-CRC], CPI-naïve pancreatic
116 cancer, and newly diagnosed high-grade gliomas after chemoradiation) [13, 27, 28].

117 The most intensively studied IL-7R agonist now in development is the PK-enhanced IL-7
118 efineptakin alfa, previously shown to suppress tumor growth in preclinical murine tumor models,
119 both as monotherapy and in combination with a PD-1 CPI. Efineptakin alfa in the clinic (as
120 monotherapy and in combination with PD-(L)1 inhibitors) is relatively well-tolerated and
121 biologically active, achieving considerable T-cell expansion with limited T_{REG} expansion.
122 Efineptakin alfa has achieved clinical responses (partial and complete) when combined with CPI
123 in immunologically cold tumor types and tumors that are relapsed/refractory to prior treatments.
124 In various clinical studies of efineptakin alfa in combination with a CPI, increased T-cell
125 proliferation in the periphery, and objective responses have been observed in immunologically
126 cold tumor types (microsatellite stable colorectal cancer, pancreatic ductal adenocarcinoma) and
127 tumor types that are relapsed/refractory to prior treatments (triple negative breast cancer, non-
128 small cell lung cancer, and small cell lung cancer)[29-33].

129 Here we describe novel agonists of the human IL-7 receptor, discovered from randomly
130 assembled peptides and unrelated to the sequence of IL-7; and we compare these surrogate
131 agonists with IL-7 in stimulating relevant T-cell subsets. The compounds discussed are a
132 synthetic 42 amino acid peptide, MDK1472, and MDK-703, a recombinant fusion of the amino
133 acid sequence of MDK1472 to an IgG2 Fc domain to extend half-life *in vivo*. We show these
134 compounds to be full agonists in inducing immune cell phenotypes that closely emulate those
135 generated by natural IL-7. The small size and low structural complexity of the pharmacologically
136 active peptide component allows facile incorporation into protein structures, such as therapeutic

137 antibodies, to combine with IL-7 agonism to create agents with new biological properties. These
138 agonist molecules score very low in predicted immunogenicity analysis; and the lack of sequence
139 similarity with IL-7 avoids the possibility of immunogenic neutralization of the endogenous
140 cytokine if an ADA response should occur.

141

Results

Peptide ligands of IL-7 receptor subunits identified and assembled into receptor agonists

The IL-7R is a heterodimer consisting of a cytokine-specific alpha chain (IL-7Rα, CD127) and the common gamma chain (γc, CD132), the latter shared by receptors of six cytokines belonging to the γc family. As is typical of hematopoietic cytokine receptors, IL-7R signaling is induced by engagement of protein agonists with both receptor subunits, either recruiting individual subunits into an oligomeric complex, or re-arranging pre-assembled subunits to correctly position the subunit-associated janus kinases (JAKs) to initiate a signaling cascade. To create molecules that emulate this agonistic mechanism, we employed an iterative process of peptide ligand identification for each of the two receptor subunits, ligand affinity enhancement, combinatorial assembly of ligand pairs into heterodimers, and functional testing of heterodimeric peptides to identify those exhibiting IL-7R agonist activity.

To identify collections of ligands binding to either human IL-7Rα or γc receptor subunits, we constructed libraries of peptides expressed on filamentous phage (each $>10^{10}$ clones per library) comprised of randomly assembled peptides, with or without positions containing fixed amino acids chosen to induce secondary structure; and these were screened for binding to the target subunit extracellular domains (ECDs), as we have previously described [34, 35]. Screening campaigns yielded distinct families of peptide ligands specific for each of the subunits. Each family was defined by a set of many sequence-related peptides, none of which exhibited sequence similarity to IL-7. Representative peptides, closely aligned with the

163 consensus sequence of each family, were chemically synthesized and tested for receptor subunit
164 binding. These initial hits bound only to the subunit from which they were recovered, typically
165 with low affinities, often weaker than 1 μM.

166 Affinity maturation of these initial families produced ligands with improved affinities
167 [34]; and combinations of these ligands (one each for IL-7Rα and γc) were joined into
168 heterodimers in a variety of orientations (i.e., joined by N-termini, C-termini, or N-to-C termini),
169 with several connection chemistries, for testing as IL-7R agonists in cell-based assays. The lead
170 peptide agonist for detailed characterization, as described here, is a fusion of peptides MDK1248
171 and MDK1188, joined with a short intervening linker to form the single-chain peptide
172 MDK1472. The sequences of the individual peptide ligands and the resulting single-chain
173 peptide agonist are shown in Fig 1. The peptides were analyzed for sequence similarity to IL-7,
174 and none was found. MDK1472 exhibited IL-7R agonist activity as a synthetic peptide.
175 MDK1472 is relatively stable when incubated *in vitro* with human or cynomolgus plasma at
176 37ºC ($t_{1/2}$ = 60 hrs and 104 hrs, respectively, S1 Fig), but its modest size (4836 Da) leaves it
177 vulnerable to rapid renal clearance and limited circulating half-life *in vivo*. To improve
178 pharmacokinetic performance, we constructed a fusion of MDK1472 to the C-termini of both
179 chains of human IgG2 Fc-domain, a compound designated MDK-703 (Fig 1C); and we have
180 shown this molecule to closely emulate the pharmacological properties of the synthetic peptide
181 MDK1472.

182 **Fig 1. Sequences and schematic structures of the compounds.** (A) Amino acid sequences of
183 MDK1248, MDK1188, and MDK1472 with intrachain disulfide bonds shown as dashed lines.
184 Schematic representations of (B) peptide MDK1472 and (C) IgG2Fc-1472 fusion MDK-703.

185 The stochastic process of discovery of MDK1472 was unbiased by information from
186 naturally occurring proteins, and led to the discovery of ligands with unique amino acid
187 sequences, unrelated to IL-7 or other proteins in the human protein sequence database. In
188 therapeutic applications, such non-self peptides have the potential for generating an immune
189 response in patients, leading to ADAs that may neutralize the activity of the drug. To estimate
190 the likelihood of this possibility, a segment of the Fc-fusion MDK-703, including the sequence
191 beginning 9 residues upstream of the linker that connects the Fc-domain to MDK1472 and
192 continuing to the C-terminus of the MDK1472 sequence was evaluated by an algorithmic
193 predictive screen for the presence of human class II (HLR "DR") restricted HLA epitopes
194 (EpiVax, Inc., EpiMatrix™ system) [36, 37]. This screen analyzes the set of nested 9-mers
195 covering the entire surveyed sequence (including linker sequences) for predicted recognition by
196 the 12 major MHC haplotypes. The low global "EpiMatrix™" score and regional analysis for
197 clusters of potential HLA-reactive segments suggest limited potential for immunogenicity (score
198 of -21.70); MDK-703 lacks evidence of putative human HLA DR epitope clusters and was
199 chosen as the lead candidate to advance into preclinical development. Because active peptide
200 constituents of MDK1472 and MDK-703 are completely novel, we have undertaken a broad
201 comparison of the functional properties of these compounds with human IL-7.

202 Binding and agonist properties of MDK1472 and MDK-703

203 IL-7R subunit binding of ligands and agonists

204 Binding affinities of peptide MDK1472 and its constituent subunit-binding fragments,
205 MDK1248 (IL-7Rα) and MDK1188 (γc), and of the Fc fusion MDK-703 to human and
206 cynomolgus subunits were determined by competition binding enzyme-linked immunosorbent

207 assay (ELISA). The IC_{50}s of MDK1248 binding human IL-7Rα ECD, and MDK1188 binding
208 human γc ECD are 150 and 24 nM, respectively (Figs 2A and 2B), and are similar to those of the
209 heterodimeric peptide MDK1472 (340 and 57 nM); while MDK-703 (presenting the
210 heterodimeric peptide on each Fc chain) binds IL-7Rα ECD and γc ECD, in this valency-
211 sensitive format, with IC_{50}s of 10 and 0.63 nM, respectively (Figs 2A and 2B). The IC_{50}s of the
212 peptide monomers, heterodimer, and MDK-703 bind to cynomolgus receptor subunits with
213 affinities within 2-fold those of the respective human subunits. Direct binding affinities of
214 MDK1472 for human IL-7Rα and γc subunits were determined by biolayer interferometry (BLI),
215 yielding K_Ds estimated to be 302 and 16.5 nM respectively, consistent with the competition
216 ELISA values (Figs 2C and 2D).

217 **Fig 2. Binding of MDK1472, MDK-703, and component peptides to human and**
218 **cynomolgus IL-7R subunits.** (A, B) Determination of IC_{50} values in a competition ELISA for
219 compound binding to human and cyno IL-7Rα and γc. The assay format is IL-7Rα-$(His)_6$-tagged
220 ECD or Fc-γc ECD immobilized on 96-well plates. Tracers are C-terminal biotinylated forms of
221 the reference IL-7Rα and γc peptide ligands, each pre-complexed with Neutravidin-HRP (NA-
222 HRP). (C, D) Label-free measurement of the equilibrium dissociation constant (K_D) for peptide
223 binding to IL-7Rα and γc extracellular domains with peptides was performed by biolayer
224 interferometry as detailed in methods. Red lines depict 1:1 binding fit from Gator™ software.
225 Blue lines represent individual BLI sensogram data taken every 0.1 seconds. Inset table displays
226 comparison of ELISA data and BLI kinetic data.

227

228 **MDK1472 and MDK-703 act directly at the receptor, binding both subunits to**
229 **induce IL-7R signaling.**

230 The synthetic peptide MDK1472 was designed to bind simultaneously to IL-7Rα and γc
231 subunits and was tested for its ability to induce phosphorylation of STAT5, the primary IL-7R
232 signaling pathway. An IL-7 responsive cell line, TF1-7Rα was constructed to express full-length
233 human IL-7Rα in TF-1 cells, which naturally express γc, but not IL-7Rα. In a STAT5
234 phosphorylation assay, MDK1472 exhibits a potency of 5 nM and full efficacy (E_{max} equivalent
235 to IL-7) (Fig 3).

236 **Fig 3. IL-7Rα dependence of agonist activity induced by MDK1472 and MDK-703 in TF-1**
237 **and TF1-7Rα cells:** Compound-induced STAT5 phosphorylation in (A) TF-1 (γc+) and (B)
238 TF1-7Rα (IL-7Rαγc+) cells. (C) pSTAT5 accumulation in TF1-7Rα cells treated with IL-7 or
239 MDK-703 in the presence of an IL-7 neutralizing antibody. Cells were pre-incubated for 15 min
240 with 1 pM to 30 nM anti-IL-7, and test compounds were then added at concentrations equivalent
241 to EC_{75} and incubated for an additional 30 min. Reactions were stopped and cell lysates prepared
242 for pSTAT5 analysis.

243 To unambiguously determine that MDK1472 acts by direct stimulation of IL-7R, we
244 compared peptide-dependent receptor activation in the TF-1 parental and TF1-7Rα cells. As
245 shown in Fig 3, agonist activity of IL-7, MDK1472, and MDK-703 are completely dependent on
246 IL-7Rα expression. In addition, we repeated the pSTAT5 assays with TF1-7Rα cells in the
247 presence of an IL-7 neutralizing antibody, showing that an antibody concentration that
248 completely inhibits IL-7 stimulation has no effect on the activity of MDK-703, ruling out the
249 possibility that IL-7R is activated by peptide-induced production of IL-7 by the cells.

250 # Receptor selectivity of MDK1472 and MDK-703

251 The cytokines and receptors of the common gamma (γc) chain family play essential roles in
252 development, homeostasis, and regulation of immunity. Each family member uniquely
253 contributes to shaping the immune response, and because each of the six receptors of the family
254 depends on the availability of γc for normal signaling, it is important to understand any effects of
255 MDK1472 and MDK-703 on the biology of the γc receptor system [38, 39]. In addition, a
256 cytokine that is not a member of the γc family, thymic stromal lymphopoietin (TSLP) utilizes the
257 IL-7Rα subunit as a co-receptor with CLRF2 (TSLPR), the private subunit of the TSLP receptor.
258 TSLP exhibits a broad range of functions, targeting both lymphoid and myeloid cells, including
259 CD4+ and CD8+ T cells, NKT, innate lymphoid 2, B cells, dendritic cells, neutrophils, mast
260 cells, eosinophils [40]. Because TSLP activity depends on interaction with IL-7Rα, we examined
261 the effect of MDK-703 on TSLP receptor-mediated events. We evaluated the potential for
262 interference by MDK1472 and MDK-703 with the signaling of cytokine receptors utilizing γc or
263 IL-7Rα subunits.

264 **MDK1472 and MDK-703 bind both subunits in the IL-7R activation complex at sites**
265 **different from IL-7**

266 To gather information on the location of the MDK1472/-703 binding sites on the IL-7R subunits,
267 we determined whether the novel agonists compete with natural IL-7 in activating the receptor.
268 Because MDK1472 and MDK-703 are themselves agonists of IL-7R, we tested the individual
269 (non-agonist) subunit binding domains of MDK1472, peptides MDK1248 and MDK1188 (Fig
270 1A), for inhibition of IL-7R-mediated receptor activation.

271 Fig 4A displays the dose-response of STAT5 activation induced by IL-7, MDK1472, and
272 MDK-703 in the IL-7 responsive cell line TF1-7Rα. This assay shows IL-7, MDK1472, and
273 MDK-703 to exhibit comparably efficacious pSTAT5 responses, with potencies ranging from 60
274 pM to 12 nM, as shown (note the individual peptide ligands MDK1248 and MDK1188 exhibit
275 no induction of pSTAT5 at 10 μM). We next treated the cells with IL-7 (at ~EC_{75}) in the
276 presence of saturating concentrations of MDK1248 or MDK1188, showing neither peptide to
277 inhibit IL-7-induced pSTAT5 accumulation, indicating that these two peptides do not compete
278 with IL-7 for binding to either receptor subunit, and that the interaction of MDK1472 (and
279 MDK-703) with each subunit of IL-7R must occur at sites independent of those bound by IL-7
280 (Fig 4B).

281 **Fig 4. Effects of MDK1472, MDK-703, and their subdomain peptides on activation of**
282 **receptors sharing subunits with IL-7R.** (A) pSTAT5 dose response of IL-7 and the test
283 compounds in TF1-7Rα cells (10 μM MDK1188 or MDK1248 alone indicated by arrow). (B)
284 Response to IL-7 in the presence of 10 μM of each of the subunit-binding peptides MDK1248
285 and MDK1188 (the peptide fragments of MDK1472, which bind to IL-7Rα and γc, respectively).
286 (C) Dose-response of IL-2, IL-4, IL-9, IL-15, and IL-21-induced STAT activation in TF-1 cells
287 expressing the respective α or β receptor subunits. Inhibition by (D) MDK1472, (E) MDK-703,
288 of the activation of each member of the γc receptor family by its respective cytokine agonist, and
289 (F) IC_{50} of MDK1188 on IL-2. (G) Dose responses of IL-7 and MDK-703 induction of pSTAT5
290 in TF-1-7Rα/TSLPR cells, and MDK-703 in the presence or absence of MDK2058, a high
291 affinity (IC_{50} = 300pM) competitive inhibitor of MDK-703 binding to the γc subunit. (H) Dose
292 response of TSLP induction of pSTAT5 in TF-1-7Rα/TSLPR cells in the presence or absence of
293 20 μM MDK2058 and 600 nM MDK-703.

294 **Effects of MDK1472 and MDK-703 on natural cytokine activation of γc family**
295 **receptors other than IL-7R**

296 The next series of experiments addressed the potential of MDK1472 and MDK-703 to interfere
297 with γc cytokine receptors of IL-2, IL-4, IL-9, IL-15, or IL-21. We constructed a set of TF-1-
298 derived cell lines, each responsive to a γc family cytokine: IL-4 (TF-1 naturally expresses both
299 γc and IL-4Rα), IL-2 and IL-15 (engineered expression of IL-2/15Rβ), IL-9 (engineered
300 expression of IL-9Rα), and IL-21 (engineered expression of IL-21Rα). Fig 4C displays the
301 potency and efficacy of phosphorylation of the appropriate STAT in each cell line upon cytokine
302 induction in the absence or presence of MDK1472 or MDK-703.

303 To assess any antagonistic effects of the test compounds, we treated each cell line with up
304 to 10 μM MDK1472 or 5 μM MDK-703 in the presence of a sub-maximal level (~EC_{75}) of each
305 cytokine. Only in the case of IL-2 stimulation of TF-1 cells expressing exogenous IL-2/15Rβ did
306 we detect any interference by the test compounds: inhibition of pSTAT5 response with an IC_{50} of
307 >5 μM (Figs 4D, E). We further determined that the IL-2R inhibition was produced by the γc
308 ligand peptide MDK1188 alone (Fig 4F), establishing that activation of IL-2βγc receptor is
309 weakly affected by MDK1472 and MDK-703 binding to γc subunit. The potency of this
310 inhibition is ~100-fold weaker than the affinity of MDK1472 (and MDK1188) for γc binding,
311 indicating that inhibition of IL-2R activation by the test compounds is not competitive with IL-2,
312 suggesting an allosteric effect on IL-2 receptor activation. Because the agonist potency of
313 MDK1472 and MDK-703 on IL-7R is 3 to 4 logs greater than its IC_{50} for IL-2R inhibition, there
314 should be no practical effect on the IL-2R system from therapeutic uses of MDK-703 as an IL-
315 7R agonist (see below). It is notable that neither MDK1472 nor MDK-703 exhibit inhibition of

316 IL-15, which shares the IL-2/15Rβγc receptor with IL-2. There is no detectable effect of the
317 novel agonists on the activation of any of the other receptors of the γc family.

318 **MDK-703 does not induce nor inhibit TSLP receptor activation.**

319 To assess the effect of MDK-703 on activity of the TSLP receptor, we prepared a TF-1-derived
320 cell line engineered to express both IL-7Rα and TSLPR. These cells, designated TF-1-
321 7Rα/TSLPR, are responsive to both IL-7 and TSLP in inducing STAT5 activation. As shown
322 above, MDK-703 binds to IL-7Rα with an affinity of 10 nM at a site not competitive with IL-7.
323 To test the effect of MDK-703 on TSLP activation of the TSLPR/IL-7Rα heterodimeric
324 receptor, a pSTAT5 dose response of TSLP in the presence of 600 nM MDK-703 (40 to 100-fold
325 the EC50 of IL-7R activation by MDK-703 in these cells) was measured. To suppress activation
326 of the IL-7 receptor in this assay, we included MDK2058, a high affinity inhibitor of the
327 interaction of MDK-703 with the γc subunit, allowing us to isolate the effect of MDK-703 on the
328 TSLP receptor. Fig 4G displays the dose response of MDK-703 ± inhibitor MDK2058, showing
329 that IL-7R activation by up to 1μM MDK-703 is fully suppressed by 20 μM of the inhibitor.
330 Furthermore, the dose response of TSLP activation is not detectably affected by the presence of
331 the γc inhibitor, MDK2058, nor by the addition of 600 nM of MDK-703. These results indicate
332 that MDK-703 does not interfere with activation of the TSLP receptor, and binds IL-7Rα at a
333 site independent of TSLP.

334 **Response of human lymphocytes to test compounds and IL-7**

335 **Comparison of the kinetics and efficacy of pSTAT5 and proliferation induced**
336 **by IL-7 and the novel IL-7R agonists in human lymphocytes *in vitro*.**

337 The most prominent lymphocyte signaling pathway induced by IL-7 is the JAK-initiated cascade
338 leading to STAT5 activation and consequent regulation of downstream transcription. We
339 analyzed STAT5 activation in isolated naive CD4+ and CD8+ T-cells to compare signaling
340 mediated by IL-7 and the test compounds MDK1472 and MDK-703. We first assessed induction
341 kinetics over a time course of compound exposure. Saturating concentrations of each of the
342 compounds, previously determined to elicit maximum response of pSTAT5 signaling, were
343 applied to the cells and pSTAT5 levels monitored for up to 2 hours. The resulting time-response
344 profiles served to compare the kinetics of signal induction for the different compounds, and to
345 determine T_{max} for correct time of exposure in subsequent dose response determinations for each
346 compound. In these studies, IL-7-induced pSTAT5 accumulation rose rapidly to a maximum by
347 15 to 30 minutes, then declined slowly for the remainder of the time course. The rate of
348 induction and T_{max} were found to be the same for IL-7, MDK1472, and MDK-703 in both cell
349 types (Fig 5A). Dose response assays, conducted at 15 minutes of compound exposure (Tmax),
350 revealed that MDK1472 and MDK-703 behave as full agonists in both cell types (Fig 5B),
351 indicating that under the conditions of these studies, STAT5 pathway activation is similar in both
352 rate of induction and efficacy upon treatment with IL-7 and the test compounds.
353 **Fig 5. MDK1472 and MDK-703 behave as full agonists in activating the JAK-STAT5**
354 **pathway.** Naive CD4+ and CD8+ T-cells, were separately isolated by negative selection from
355 PBMCs, and rested overnight prior to compound exposure. (A) Cells were treated with saturating
356 concentrations of IL-7 (10 nM), MDK1472 (1 μM), and MDK-703 (1 μM) for up to 2 hours and
357 scored for pSTAT5 accumulation by ELISA. (B) The dose response for each compound was
358 measured in human naive CD4+ and CD8+ cells, utilizing an exposure time of 15 min (T_{max}).

359 **MDK-703 exhibits cell selectivity similar to IL-7 in stimulating signaling and**
360 **proliferation in major human T-cell populations**

361 IL-7 exerts a broad range of effects on the lymphoid system, as most mature T-cells exhibit some
362 IL-7Rα expression, with surface levels of IL-7Rα subunits and biological response to IL-7
363 fluctuating with the environment and differentiation status of the cells. To compare cell
364 selectivity of MDK-703 with IL-7, we followed compound-mediated phosphorylation of STAT5
365 in major peripheral T-lymphocyte subpopulations of rested and CD3/CD28-activated PBMCs
366 from 5 healthy donors following exposure to the compounds. Fig 6 displays dose-response
367 curves for both compounds, assessed by flow cytometry of pSTAT5 gated on CD8+ and CD4+
368 T-cells, CD4+ regulatory T-cells (Treg), and NK cells. In each population, when rested or
369 activated, the potency of IL-7 is significantly higher, but the efficacy (E_{max}) of MDK-703 or IL-7
370 is the same, demonstrating that MDK-703 behaves as a full agonist of pSTAT5 activation in
371 lymphocytes (Figs 6A and 6B). Consistent with the known functions of IL-7 agonists, both
372 compounds induce the most robust pSTAT5 induction in CD4+ and CD8+ cells, with a
373 significantly lower response in Tregs, cells that typically express low levels of IL-7Rα [41, 42].
374 Also as expected, NK cells show no pSTAT5 response to either IL-7 or MDK-703.

375 We also evaluated pSTAT5 signaling in PBMCs of cynomolgus macaques, with results
376 similar to the human studies: MDK-703 activated IL-7 receptor signaling in CD8+ and CD4+ T-
377 cells, less in Tregs, and showed no activation of NK cells from the rested cynomolgus monkey
378 PBMCs. Each compound exhibits potency comparable to that seen in human lymphocytes. As
379 was the case with human PBMCs, both MDK-703 and IL-7 exhibit equivalent efficacy in

380 cynomolgus lymphocyte subtypes (Fig 6C). These results demonstrate that MDK-703 is a full
381 agonist of IL-7R with cell selectivity similar to that of IL-7.

382 **Fig 6. Induction of pSTAT5 in PBMCs treated with MDK-703 or IL-7**. Frozen PBMCs from
383 5 healthy human donors (A, B) and cynomolgus monkey (C) were rested (A, C) or activated with
384 anti-CD3/CD28 (B). Cells were stained for viability, followed by cell surface antibody staining
385 on ice. Cells were washed and incubated with MDK-703 or IL-7 for 30 min at 37ºC to activate
386 the IL-7 receptor. After washing, cells were fixed, permeabilized, stained with anti-pSTAT5
387 antibody, and analyzed immediately by flow cytometry. The mean fluorescence intensity (MFI)
388 of pSTAT5 detection was shown as mean ± SEM. (D), EC_{50} values of MDK-703 vs. IL-7 in
389 immune subsets in human and cynomolgus PBMCs are shown in S1 Table. Flow cytometry
390 gating data shown in S2 Fig.

391

392 An essential feature of IL-7-mediated homeostatic lymphoid maintenance is the
393 proliferation of naive T-cells, expanding both recent thymic emigrants and circulating T_N clones
394 to sustain the population and preserve a diverse TCR repertoire in the naive T-cell compartment.
395 Memory T-cells require periodic IL-7 stimulation for long-term maintenance of the population
396 and the potential for rapid expansion in response to antigen re-stimulation [43-45]. We treated
397 rested PBMCs with MDK-703 or IL-7 (at E_{max} based on pSTAT5 dose-response) and determined
398 Ki-67 levels, a marker of proliferative potential, and cell numbers of the major lymphocyte
399 populations by flow cytometry (Fig 7). We found Ki-67 induction in each of the scored cell
400 subsets to be similar upon treatment with MDK-703 or IL-7. In the CD8+ population, Ki-67+
401 frequency reached a peak by day 7, declining slightly by day 16. CD4+ T-cells exhibited a

402 somewhat lesser response which was maintained to day 16. CD4+ Tregs, which typically express
403 less IL-7Rα and are less sensitive to IL-7, displayed a significant rise in Ki-67 induction, but
404 over a strong background of Ki-67 increase in the untreated cells. NK cells also exhibited a
405 response profile similar to that of the CD4+ T-cell population; and as with Tregs, NK exhibited
406 high Ki-67 background in untreated cells. The high Ki-67 background in untreated samples of
407 Treg and NK cells may indicate a high basal turnover rate of these cell types in culture [46].
408

409 **Fig 7. Proliferation of PBMC subpopulations following treatment with MDK-703 or IL-7**.
410 Frozen PBMCs from 5 healthy donors were rested overnight and treated with 100 nM MDK-703
411 or 1nM IL-7, or no added compound, and cultured for 30 days in the presence of compounds. On
412 days 3, 7, 16, and 30, cell aliquots were taken and analyzed by flow cytometry for (A) Ki-67
413 expression and (B) absolute numbers of $CD8^+$, $CD4^+$, Treg, and NK cells. Data are shown as
414 mean ± SEM. Flow cytometry gating data shown in S2 Fig.

415 In following treatment-dependent expansion of CD8+ and CD4+ T populations, we found
416 CD8+ T-cell numbers were not increased by day 7 but exhibited strong expansion between days
417 7 and 16 of compound exposure and continued to increase through day 30 in culture, resulting in
418 4.3-fold (MDK-703) and 5.2-fold (IL-7) increases over baseline. The CD4+ T-cell population
419 also expanded with similar kinetics, but with lower fold-increase over baseline by 30 days of
420 compound exposure.

421 In the untreated samples, both CD8+ and CD4+ T-cell numbers declined over time. In the
422 presence of the compounds, a slight increase in Treg cell numbers was observed; and NK cells
423 showed no evidence of population expansion in this experiment, a result consistent with the
424 known low response of NK cells to IL-7R agonists.

425

426 **MDK1472 and MDK-703 induce IL-7Rα internalization with kinetics similar**

427 **to IL-7**

428

429 Upon binding to its receptor, IL-7 induces both signaling, and internalization of the active
430 receptor complex. CD8+ cells in the absence of IL-7 continuously internalize IL-7Rα at a low
431 rate via endosomal uptake with recycling to the cell surface; However, in the presence of IL-7
432 clathrin-mediated uptake of the signaling complex increases substantially, with IL-7Rα directed
433 to late endosomes and targeted for proteasomal degradation [47, 48]. This reduces IL-7Rα
434 surface expression and lowers cell responsiveness to IL-7. Internalization of the ternary signaling
435 complex also depletes the local milieu of IL-7, an effect described as the "consumption" model
436 of IL-7-mediated T-cell homeostasis [10, 11].
437 Because of the importance of IL-7Rα internalization and IL-7 consumption in modulating T-cell
438 homeostasis, we evaluated the kinetics of receptor internalization induced by MDK1472 and
439 MDK-703 in rested human CD8+ cells compared with IL-7 treatment. In previous studies, the
440 decline of IL-7Rα on the surface of IL-7-treated CD8+ cells was reported to proceed with
441 approximately linear kinetics, reaching ~80% disappearance of receptor over 6 hours at 37°C
442 [47]. We performed a similar experiment, tracking CD8+ surface IL-7Rα with a labeled anti-
443 CD127 (IL-7Rα) antibody that we showed not to compete with either IL-7, MDK1472, or MDK-
444 703 in binding and detecting the receptor subunit (S3 Fig). Surface IL-7R was pre-loaded with
445 saturating concentrations of the agonists on ice and shifted to 37°C to allow internalization, then
446 shifted back to ice to stop internalization. Negative controls consisted of untreated (no compound

447 added); MDK1169, a peptide agonist of another γc family receptor (which contains a γc binding
448 domain similar to MDK1472 but lacking the IL-7Rα binding domain); and MDK-202, an Fc-
449 fusion of MDK1169 (a construct analogous to MDK-703, with the same Fc domain fusion
450 partner). A parallel assay with all incubations held on ice for the duration of the time course was
451 also run.
452
453 As shown in Fig 8 (and S3 Fig), IL-7 induces a temperature-dependent decline in IL-7Rα
454 surface density, reaching a loss of 60% at 6 hours, consistent with the results of Faller, et *al.*[47].
455 The rate of surface decline of IL-7Rα upon treatment with MDK1472 or MDK-703 tracked very
456 closely with that induced by IL-7. The negative control samples exhibited no IL-7Rα uptake at
457 37°C; and all samples held under cold conditions showed no change in IL-7Rα surface density.
458 These observations are consistent with the interpretation that IL-7Rα disappearance from the cell
459 surface upon treatment with these agonists is the result of cellular internalization, and the
460 conclusion that MDK1472 and MDK-703 induce the uptake of IL-7Rα in rested CD8+ cells at a
461 rate, and to an extent essentially identical to that driven by IL-7.
462
463 **Fig 8. Test compounds induce decrease in cell surface IL-7Rα.**
464 Rested human CD8+ T-cells were treated with saturating concentrations of the test agonists (10
465 nM IL-7; 1 μM MDK1472 or MDK-703) or the negative control compounds (untreated, 1 μM
466 MDK1169, or MDK-202) for 20 minutes on ice, then incubated at (A) 37°C or (B) 0°C for
467 varying times to monitor uptake of IL-7Rα from the cell surface. Following timed incubations,
468 the samples were stained, fixed, and analyzed by flow cytometry; and data was collected as
469 median fluorescence intensity (MFI), as detailed in Methods. These data were normalized with

470 the blank value (no added compound) set at 100% surface IL-7Rα, and the signal baseline set at
471 0. The primary flow data (MFI) is shown in S3 Fig.
472

473 Effects of IL-7 and MDK-703 on T-memory subpopulations

474 MDK-703 drives expansion of naïve and memory T-cell subpopulations in 475 human PBMCs

476

477 Naive and memory subsets of peripheral T-cells are highly responsive to IL-7 by virtue of
478 robust expression of IL-7Rα. We compared the effect of IL-7R agonists IL-7 and MDK-703 on
479 CD8+ T-memory subpopulations in rested human PBMCs, and found the effect of MDK-703 on
480 cell number to be similar to that of IL-7 on T-naïve and on all Tmem populations observed (Fig
481 9). Treatment with both compounds caused an immediate decline in CD8+ naive cells, reaching a
482 nadir by day 7, followed by a return to initial levels by day 16 that were sustained to the end of
483 the 30 day duration of the experiment. In contrast, memory T cell populations were low at T_0 and
484 exhibited little or no initial dip, followed by substantial increase in cell count by day 16 of
485 exposure to the compounds. Most notable is the behavior of a very early effector/memory subset
486 designated T-stem cell memory (Tscm), a cell type exhibiting persistent stem-like properties (Fig
487 9B). Both MDK-703 and IL-7 drive an increase in CD8+ Tscm cell number beginning day three,
488 and a dramatic population expansion to reach a 1300-fold increase by day 30, compared to a 5-
489 fold expansion in the untreated group. The remaining memory populations exhibited more
490 modest (fold) increases in cell number following exposure to either IL-7 or MDK-703. CD8+
491 central memory (Tcm) exhibited a modest initial decline, then a rapid rise to a peak by day 16 of

492 5- to 6-fold over day 0, followed by a slight decline by day 30 to 3- to 4-fold elevation over day
493 0. Similarly, CD8+ effector memory (Tem) exposed to the IL-7R agonists exhibited a small early
494 decline but increased 3- and 4-fold by day 16, a level which persisted until day 30. CD8+
495 terminally differentiated effector memory cells (Temra) responded to IL-7 and to MDK-703 with
496 marked expansion of 7- and 11-fold over 30 days. For naïve and all memory populations, cells
497 showed little evidence of expansion in the absence of IL-7R agonists (untreated) These results
498 demonstrate MDK-703 to be as effective as IL-7 in stimulating memory T cell expansion, in
499 particular the stem-like Tscm population (Figs 9B and 9C). The profound effect of both IL-7 and
500 MDK-703 on the cell number of the overall memory compartment as well as the individual
501 subpopulations is illustrated in the histograms shown in Figs 9D and 9E.
502
503 **Fig 9**. **The expansion of CD8+ T memory subpopulations following treatment with MDK-**
504 **703 or IL-7**. Frozen PBMCs from 5 healthy donors were rested overnight and left untreated or
505 treated with 100 nM MDK-703 or 1 nM IL-7 in culture. On days 3, 7, 16, and 30, cell aliquots
506 were taken and analyzed by flow cytometry of CD8+ T naïve and memory populations. (A)
507 Schematic of the putative differentiation pathway of the memory T cell compartment. (B)
508 differential gating of naïve and early memory (Tscm) subpopulations. (C) Cell counts of treated
509 and untreated memory subpopulations over time. (D) Stacked bar representation of changes in
510 total memory T cell subpopulations over time. (E) Comparison of CD8+ Tscm expansion on day
511 16 and day 30 of culture with MDK-703 or IL-7. Data are shown as mean ± SEM. Detailed
512 gating information is provided in S4 Fig.
513
514 **MDK-703 drives expansion of immune cells in huCD34^{+}-engrafted NSG mice**

515 MDK-703 binds and activates both human and NHP IL-7 receptors but is inactive on the murine
516 receptor. To evaluate the effects in a rodent model, we utilized NSG mice engrafted with human
517 CD34+ hematopoietic stem cells (CD34+ HIS mice) (Fig 10). Mice were administered a single
518 intravenous dose of human Fc isotype control or MDK-703 at 1 mg/kg. Peripheral blood samples
519 were analyzed on day 7, and terminal blood and splenocytes were analyzed on day 12 .
520 Consistent with the pSTAT5 induction data, MDK-703 increased the Ki-67+ population in
521 peripheral CD8+ and CD4+ T-cells, but not in Tregs or NK cells on day 7 (Fig 10B); however, at
522 this time point, cell numbers were not increased over the Fc control group (S5 Fig). On day 12,
523 Ki-67+ cells were no longer observed (S5 Fig), but CD8+ and CD4+ T-cell numbers were
524 elevated (Fig 10C). In vivo, both Treg and NK cell numbers, typically unresponsive to IL-7
525 agonists, were increased, suggesting an indirect effect of MDK-703, possibly driven by IL-7R-
526 dependent release of cytokines in the engrafted immune system.

527 **Fig 10. Expansion of immune cell subpopulations in humanized mice treated with MDK-**
528 **703**. NSG mice (n=10 per treatment) engrafted with human CD34+ cells from two donors (5
529 mice/donor) were dosed once intravenously with 1 mg/kg Fc (gray bars) or MDK-703 (blue
530 bars), and peripheral blood (B-D) and spleen (E-G) were collected and analyzed at the indicated
531 times by flow cytometry. (A) Diagram of the experimental plan. (B) Frequencies of Ki-67+ in
532 CD3+, CD4+, CD8+, Treg, and NK cell populations in peripheral blood on day 7. (C) Absolute
533 cell numbers of CD3+, CD4+, CD8+, Treg, and NK cell populations in peripheral blood on day
534 12. (D) CD8+ T memory subpopulations in peripheral blood on day 12. (E) Absolute cell
535 numbers of CD3+, CD4+, CD8+, Treg, and NK cell populations in the spleen on day 12. (F)
536 CD8+ T memory subpopulations in the spleen on day 12. (G) TCF1 expression in CD8+ T
537 memory subpopulations in the spleen on day 12. Population gates were drawn based on FMO

538 controls. Statistical analysis was done using Student's T-Test. *p<0.05, **p<0.005, and
539 ***p<0.0005. Detailed gating information is provided in S6 Fig.

540 The CD8+ Tn and Tcm compartments showed elevated frequencies of Ki-67+ cells on
541 day 7 (S5 Fig), and Tn, Tscm, and Tcm cell numbers expanded in response to MDK-703; but
542 Tem and Temra did not reach significance – an observation possibly due to the limited time
543 course of this experiment, as we had observed a robust in vitro expansion of Tem and Temra
544 from PBMC in 16 to 30 days of culture (see Fig 9).

545 More dramatic changes were observed in the spleen. Absolute cell numbers were
546 significantly increased in CD8+, CD4+ T-cells, Treg, and NK cell populations (Fig 10E) without
547 changes in the Ki-67+ except for CD4+ T-cells (S5 Fig) by MDK-703. The effect on NK cells is
548 assumed to be a secondary or indirect effect of MDK-703 treatment. CD8+ naïve and memory
549 subpopulations were expanded to a greater extent in the spleen than in blood by 12 days of
550 treatment with MDK-703 (Fig 10F). We observed Tn, Tscm, Tcm, and Temra, to be significantly
551 expanded (Tem did not reach significance). T-cell factor 1 (TCF1) transcription factor is
552 expressed in self-renewing immune cells. Since TCF1+ expression is found in naïve and Tscm
553 cells, we examined the effect of MDK-703 on TCF1+ cell expansion. As shown in Fig 10G,
554 MDK-703 treatment increased TCF1 frequency in CD8+ Tn and Tscm, which are highly
555 proliferative and less differentiated, less in Tcm; but non-significant in Tem and Temra, cells
556 which are more differentiated and have lower proliferation capacity. The results indicate that
557 MDK-703, like IL-7, drives a substantial increase in stem-like memory cells.

558 **MDK-703 in non-human primates**

559 **MDK-703 exhibits an extended circulating half-life and induces persistent**
560 **elevation of peripheral lymphocytes in non-human primates**

561 MDK-703, an Fc-fusion designed to extend the half-life of the pharmacologically active IL-7
562 agonist peptide MDK1472, was administered as a single dose of 1 mg/kg to naive cynomolgus
563 macaques via intravenous, subcutaneous, or intramuscular injection. MDK-703 was well
564 tolerated, with no adverse effects on clinical observations or blood chemistry.

565 The mean terminal half-life of MDK-703 was 46 hours in these animals, with higher
566 bioavailability achieved after subcutaneous or intramuscular injection (Fig 11A). In a separate
567 study, three animals were dosed once subcutaneously with 0.3 mg/kg and observed for changes
568 in absolute lymphocyte count (ALC, hematology) and the expansion of CD8+, CD4+, Treg, and
569 NK cells (by flow cytometry) for up to 42 days. Following administration, absolute lymphocyte
570 (ALC) counts dropped from baseline to a nadir at 1-2 days, recovering to baseline by day four
571 and reaching a peak of ~130% over baseline by day 10 (Fig 11B). ALC remained elevated
572 through day 29, and slowly declined to near baseline level by day 41, demonstrating that the
573 MDK-703 pharmacodynamic effect persists well beyond the exposure to treatment. The initial
574 drop in cell number was observed in CD8+ and CD4+ T-cells, peaking on day seven and
575 remaining elevated (>50% over baseline) for 29 days (Fig 11C). There was no significant
576 increase in Treg count, consistent with the data from CD34+ humanized mice. The initial drop in
577 blood lymphocytes following IL-7R agonist administration is attributed to the induction of
578 adhesion molecule expression directing the uptake of responding cells into tissues [49].
579 Proliferation and expansion of lymphocytes then follow, with a duration of effect well beyond
580 the circulating persistence of the compounds, consistent with the known protective, anti-

581 apoptotic properties of IL-7R agonists in extending T-cell lifetime [50]. These results are similar
582 to those reported in patients treated with a PK-stabilized formulation of IL-7 (GX-17; IL-7 fused
583 to an Fc-domain) [25].

584 **Fig 11. Pharmacokinetic (PK) and pharmacodynamic (PD) properties of MDK-703 in**
585 **cynomolgus macaques.** (A) PK of MDK-703: Animals (n=3) were administered a single dose of
586 1 mg/kg MDK-703 via IV, SC, or IM. The serum concentration of MDK-703 at the indicated
587 time points was determined by sandwich ELISA. (B and C) PD effect of MDK-703: Three
588 animals were dosed once subcutaneously with 0.3 mg/kg, and blood samples were collected at
589 the indicated time points for absolute lymphocyte counts (B) and immune profiling of CD8,
590 CD4, Treg, and NK cells by flow cytometry (C). Data show mean ±SEM.

591

592 # Discussion

593 MDK-703 is the fusion of a structurally novel IL-7 peptidyl agonist with an huIgG2-Fc domain.
594 The peptide component, MDK1472, was assembled as a single chain heterodimer of novel
595 peptide ligands of IL-7Rα and γc joined by a short flexible amino acid linker. A notable feature
596 of the active agonist peptide is the stochastic process of discovery of the component ligands,
597 leading to an IL-7R agonist completely unrelated in sequence to native IL-7. We found
598 MDK1472 to exert receptor agonism through binding to sites distinct from the binding sites of
599 IL-7 on both receptor subunits. Although the relative affinities of MDK1472 for IL-7Rα and γc
600 differ from that of IL-7, signal transduction initiated by the formation of a ternary complex with
601 both receptor subunits is similar to that of IL-7.

602 The novel sequence of the active peptide provides distinct benefits over natural IL-7 as a
603 therapeutic agent. Various forms of IL-7 modified for clinical applications exhibit immunogenic
604 properties, including induction of antibodies which neutralize IL-7 activity [25]. Such IL-7
605 neutralizing antibodies have the potential to affect endogenous IL-7, which can produce
606 significantly detrimental effects in patients. The small size of the peptide component of MDK-
607 703 reduces the likelihood of harboring immunogenic epitopes, and *in silico* algorithms predict a
608 very low propensity for immunogenicity. Furthermore, should an immunogenic response to the
609 novel peptide sequence occur, ADAs would not neutralize endogenous IL-7. The single chain
610 peptidyl structure of the peptide also provides a means of pharmacokinetic enhancement by
611 fusion to an Fc partner; and the Fc -fusion MDK-703 exhibits substantial persistence in the blood
612 of non-human primates after IV, IM, and SC administration.

613 Some studies on the clinical use of agonists derived from natural IL-7 report injection site
614 reactions in patients. These effects may be explained by the reported binding of IL-7 to
615 components of the extracellular matrix, potentially resulting in injection site depot effects [4, 51].
616 In addition, recombinantly expressed proteins occasionally form aggregates, as exemplified in
617 the report of a fusion of IL-7 to IgG-Fc [52]. Although formulations can be employed which
618 limit this effect, subsequent injection of high concentrations of formulated drug into
619 physiological aqueous environments may induce aggregation and local deposition. MDK-703
620 injected SC or IM into NHP, exhibited systemic bioavailability similar to that produced by IV
621 dosing. Preliminary assessment of MDK-703 dosed IM in healthy human subjects found no
622 injection site reactions, and systemic MDK-703 exposure consistent with that predicted from
623 NHP studies, suggesting high bioavailability in humans [53].

624 Because the peptidyl agonist component of MDK-703 is not naturally occurring, is
625 unrelated to IL-7, and acts through a unique binding complex with IL-7R, we undertook a
626 detailed comparison of receptor signaling and cellular responses induced by the synthetic
627 peptide, the Fc-fusion, and IL-7. We showed MDK1472 and MDK-703 to activate the IL-7R
628 through direct receptor interaction to faithfully emulate the kinetics and efficacy of IL-7
629 internalization, signal transduction, and stimulation of proliferation in human lymphocyte
630 subpopulations. At concentrations that produce maximal IL-7R-mediated pSTAT5 elevation,
631 neither MDK1472 nor MDK-703 significantly affected the activity of any other γc cytokines at
632 their respective receptors.

633 To compare the biology of MDK-703 with IL-7, we measured pSTAT5 in the major
634 lymphocyte subtypes CD4+, CD8+, CD4+Tregs, and NK cells in human and cynomolgus
635 PBMCs; and found that the kinetics and Emax of pSTAT5 induction in each subtype is

636 essentially the same for both MDK-703 and IL-7, and this finding held for PBMCs of both
637 species. CD4+ and CD8+ cells exhibit the most robust response to the compounds, followed by
638 more modest effects on CD4+Tregs, and very little response in the NK population -- results
639 consistent with previously described properties of IL-7R agonists. With respect to Tregs, IL-7R
640 agonists have been reported to reduce their immunosuppressive properties [41, 54], potentially
641 enhancing the therapeutic utility of MDK-703 in oncology and infectious disease.

642 The *in vitro* potency of MDK-703 in the pSTAT5 assay is 10 to 100-fold lower than that
643 of IL-7. In some cases, attenuation of the potency of cytokine derivatives has been shown to
644 increase the availability of drugs that are subject to target receptor-mediated disposition (TMDD)
645 [55]; and we previously reported that the potency of MDK-703 is sufficient to achieve robust PD
646 effects on blood T-cells at doses as low as 30 µg/kg IM in healthy human subjects [53].

647 In addition to *in vitro* pSTAT5 phosphorylation, we showed both MDK-703 and IL-7 to
648 induce similar expansion of lymphocyte numbers in culture: CD4+ and CD8+ cells reached
649 maximal counts 5-fold over day 1 baseline levels between days 7 and 16, levels which persisted
650 for at least 30 days.

651 The effects of IL-7R agonists on naïve and memory T-cell compartments are well known
652 and are critical for the central role of IL-7 in maintaining a healthy immune response. Exploring
653 compound-dependent effects on these lymphocytes, we compared MDK-703 with IL-7 on rested
654 human PBMCs and found the proliferative effects on each scored subpopulation to be very
655 similar for both compounds. Focusing on CD8+ cells, we observed the number of naïve cells to
656 decline quickly and substantially, reaching a nadir by day 7, followed by a return to day 0 basal
657 level, which was sustained to day 30. In contrast, the memory T-cell populations (Tscm, Tcm,
658 Tem, Temra) all exhibited expansion of their initial cell number, with the most prominent effect

659 an early and dramatic increase of Tscm cells, a memory phenotype exhibiting evidence of both
660 activation and persistent stem-like properties. Both compounds drove the immediate increase of
661 Tscm number to reach an expansion of 1300-fold by day 30. More modest increases of Tcm and
662 Tem numbers followed a slightly delayed time course, reaching 5 to 6-fold and 3 to 4 -fold over
663 baseline, respectively, by day 16. These results demonstrate MDK-703 to be at least as effective
664 in stimulating Tmem – particularly Tscm – expansion as IL-7; and serve as further evidence of
665 the similarity in T-cell immuno-biology produced by these two IL-7R agonists *in vitro.*

666 MDK-703 exhibits substantial proteolytic stability in plasma *in vitro*, and persistence
667 after administration to NHP with circulating $T_{1/2}$ of 46 hrs. Administration by the IM and SC
668 routes demonstrated an MDK-703 AUC similar to that of IV administration.

669 MDK-703 is active on primate IL-7 receptors but exhibits undetectable activity on rodent
670 receptors. To study the pharmacodynamic properties on human immune cells, we utilized an *in*
671 *vivo* model huCD34+ engrafted NSG HIS mice. A single IV dose of MDK-703 increased the
672 frequency of Ki-67+ CD4+ and CD8+ T cells, but not Tregs nor NK cells, by day 7. On day 12,
673 Ki-67+ cells were no longer present in the peripheral CD8+ and CD4+ populations, but the cell
674 numbers were significantly increased. In these *in vivo* experiments, Tregs and NK cells, typically
675 relatively unresponsive to IL-7R agonists, were modestly elevated. This expansion may be an
676 indirect effect of L-7R-dependent release of cytokines other than IL-7, that stimulate these
677 populations. Scoring for the Tn and Tmem subsets in blood showed CD8+ Tscm and Tcm cells
678 to exhibit an increase in frequency of Ki-67+ expression at day 7, while Tn, Tem, and Temra did
679 not. By day 12, the absolute cell numbers in Tn and all Tmem compartments were significantly
680 increased in blood, and substantially elevated in spleen. The frequency of TCF1+ cells increased

681 significantly in Tn, Tscm,Tcm, and Tem, These results demonstrate that MDK-703, like IL-7,
682 drives a general increase in the number and "stemness" of memory cells.

683 In cynomolgus macaques, a single SC dose of 0.3 mg/kg produced an initial drop in
684 blood lymphocytes, characteristic of the tissue trafficking effects of IL-7R agonists, followed by
685 a return to baseline by day 4, and climbing to 230% of baseline by Day 11. This level remained
686 elevated through day 29, and declined slowly thereafter to baseline at day 41, indicating
687 persistence of the expanded lymphocytes well beyond the period of exposure to the compound.

688 Stimulation of the memory T-cell compartments appears to be of importance for the
689 reported anti-tumor activities of IL-7R agonists, either administered to animals or patients; or
690 treatment of engineered T-cells undergoing *ex vivo* expansion prior to transfer to patients.
691 Amplification of Tscm, a naive-like, but antigen-experienced population that retains a minimally
692 differentiated and highly proliferative self-renewal phenotype, appears to be a particularly
693 important subset of the T-memory compartment in this regard. As a source of potent effectors
694 resistant to antigen-driven exhaustion, cells of the Tscm subtype are predicted to exert a key
695 influence on T-cell-mediated anti-tumor immunity. In animal tumor models, both CD4+ and
696 CD8+ Tscm are implicated in anti-tumor efficacy; in humans, administration of CAR-T cells
697 with enhanced Tscm phenotype leads to improved persistence of the engineered cells, as well as
698 improved clinical outcome; and in healthy individuals Tscm exhibit greater proliferation and
699 cytotoxic polyfunctionality with a higher frequency of the triple positive effector phenotype --
700 elevation of IFNγ, IL-2, and tumor necrosis factor (TNF)α secretion -- upon secondary antigen
701 response, than do other Tmem-subsets [13-15, 27, 56-58].

702 MDK-703, the novel IL-7R agonist described here, produces strong stimulation of Tscm
703 production in PBMC cultures, and rapid appearance in both blood and spleen of MDK-703

704 treated HIS mice. This property of MDK-703 appears to be translatable to humans, as a single
705 dose of 30 μg/kg of MDK-703 in healthy subjects resulted in a 9-fold increase in CD8+ Tscm.
706 [53]. The ability to increase the Tscm population may be an important attribute of the therapeutic
707 utility of MDK-703.

708 In summary, MDK-703 exhibits properties that make it a strong candidate for clinical
709 evaluation. These include its novel chemical composition to avoid IL-7 neutralizing immune
710 response, high bioavailability, and extended half-life. Despite its novel composition and unique
711 ternary complex with IL-7Rα and γc, MDK-703 appears to faithfully emulate the properties of
712 IL-7 with respect to cellular signaling and *in vivo* expansion of T-cell subpopulations. Given the
713 unique pharmacology of MDK-703, it may have utility in indications where its
714 pharmacokinetics, lack of IL-7 neutralizing antibodies, and T-cell enhancing properties are
715 beneficial, including oncology, anti-viral and other infectious disease, vaccine enhancement, and
716 treatment of lymphopenia.

717

718 # Materials and Methods

719 ## Ethics statements

720 ***Human primary tissue samples (PBMCs)***

721 Buffy coats, PBMCs, and isolated PBMC subsets were obtained from the Stanford Blood Center
722 (Stanford University, Stanford CA) collected under eProtocol "Minimal Risk Research Related
723 Activities at Stanford Blood Center" (SQL 79075) #13942; IRB (registration 5236). Samples
724 were collected with written donor consent and anonymized prior to provision for research
725 purposes. Stanford University is in compliance with requirements for protection of human
726 subjects, including 45 CFR 46, 21 CFR 50 and 56, and 38 CFR 16.

727 Human PBMCs were obtained from Stemcell Technologies (Vancouver, BC). Samples were
728 collected from donors and anonymized prior to providing for research purposes. Stemcell
729 Technologies provided Institutional Review Board (IRB)-approved consent forms and collection
730 protocols for all lots of PBMCs used in these studies: "Leukapheresis Sample Collection from
731 Healthy Human Donors for the Purpose of Scientific and Medical Research and education" (IRB
732 protocols 2019110, 018-V.1; 018-V.7; 018.V.11; including written consent forms U5 and U9).

733 ***Human-derived established cell lines***

734 Human-derived cell lines used in this study were initially obtained from accredited commercial
735 suppliers: (1) HEK293 (human embryonic kidney cell line, FreeStyle® 293-F) was obtained
736 from Invitrogen (San Diego, CA) for use as a recombinant protein expression vehicle; and (2)
737 TF-1 erythroblast cell line was obtained from the American Type Culture Collection (ATCC
738 Cat# CRL-2003) for use as the parental cell line for the engineered expression of each full length

739 private receptor (alpha or beta) of the gamma common family, and CFLR2. No cell lines were
740 prepared directly from human tissue at Medikine.

741 ***Mouse Studies***

742 Mouse PK and PD studies were carried out at Crown Bioscience (San Diego, CA) in strict
743 accordance the regulations of the Association for Assessment and Accreditation of Laboratory
744 care (AAALAC). The study protocol was approved by the Committee on the Ethics of Animal
745 Experiments of Crown Bioscience (Protocol number CDSD-ACUP-002). The subject animals
746 (HuCD34+ humanized mice (NSG™ NOD.Cg-Prkdcscid Il2rgtm1Wjl, Stock No.005557) were
747 provided directly to Crown BioScience by The Jackson Laboratory (Bar Harbor, ME).

748 ***Non-human primate studies***

749 NHP (cynomolgus macaque) studies 2006 and 2102 were performed according to Primate
750 Products, LLC (Miami, FL) Standard Operating Procedures, authorized veterinary standards and
751 the present protocols. The protocols were approved by the Envol Biomedical IACUC (Naples,
752 Fl) (Study 2006 Approval number 7117-21; Study 2102 approval number 7174-21). Prior to
753 initiation, all animals underwent a physical examination by the study veterinarian. Upon study
754 completion, the animals were placed in the stock colony of non-naïve animals held at Primate
755 Products, LLC (PP LLC).

756 <u>Housing, feeding, and environmental enrichment</u>: Purina 5049 was provided daily in amounts
757 appropriate for the size of the animal. Tap water was provided *ad libitum* via an automatic
758 watering device. The animals were housed according to Primate Products, LLC (PP LLC)

759 standard operating procedures. Each animal's immediate holding cage was cleaned once daily.
760 Enrichment was provided as needed.

761 Humane endpoints: No humane endpoints were included in this study. The study was designed to
762 evaluate pharmacokinetics and pharmacodynamics. Animals were observed twice a day until the
763 end of the study and returned to the stock colony.

764 Preparation of compounds: Peptides and Fc-fusions

765 ***Synthesis of peptides***

766 All peptides (MDK1472, MDK1188, MDK1248, MDK1169, MDK2058) were synthesized using
767 standard Fmoc/HATU/TFA synthesis protocols. For peptides containing two cysteines, the single
768 disulfide bond was formed using trityl protection for the thiols and dimethyl sulfoxide (DMSO)
769 oxidation. For peptides containing four cysteines, and with the potential of forming three
770 disulfide bond arrangements, orthogonal protecting groups were used for the two pairs of
771 cysteines to ensure formation of only the desired disulfide bridges: one cysteine pair protected
772 with trityl and oxidized with DMSO, and the second pair protected with Acm and oxidized with
773 iodine. Peptides were purified by preparative reverse phase HPLC ($\geq$95%), and correct mass
774 verified by ESI-MS.

775 ***Preparation of MDK-703***

776 A mammalian expression vector was constructed to express peptides linked to Fc-fragments
777 consisting of the CH2 and CH3 domains of the heavy chain and hinge regions of human IgG2 Fc
778 modified as follows: The first and second cysteines of the hinge region were replaced with serine
779 to prevent detrimental disulfide bridge formation; the last amino acid (lysine) of the Fc region
780 was replaced with an alanine for fusion stability. This vector contains the strong constitutive

781 cytomegalovirus (CMV) promoter, and an IL-2 signal peptide sequence for secretion of the
782 fusion protein. To express MDK-703, a synthetic DNA fragment was inserted into the vector to
783 fuse MDK1472 to the C-terminus of the IgG2 Fc chain with a $(Gly\text{-}Ser)_{10}$ linker between the
784 peptide and the Fc domain. Fusion proteins were transiently expressed in 293 human embryonic
785 kidney cells (FreeStyle® 293-F) by transfecting plasmid DNA into the cells using
786 polyethyleneimine reagent PEI MAX (Polysciences, Inc.). Transfected cells were grown in
787 FreeStyle® 293 Expression Medium (ThermoFisher) in shaker flasks in a 37°C humidified CO_2
788 incubator on an orbital shaker rotating at 130 rpm. Cultures were harvested 96 h post-
789 transfection by centrifugation, and the secreted fusion proteins were purified from the
790 supernatants using MabSelect SuRe Protein A affinity columns (Cytiva). The columns were
791 washed with phosphate buffered saline (PBS) and the retained Fc-peptide fusion was eluted with
792 0.1 M glycine buffer (pH 2.8). Eluates were neutralized with 1 M Tris buffer and quantified by
793 measuring absorbance at 280 nm with a NanoDrop® spectrophotometer. Protein concentrations
794 were determined using calculated extinction coefficients derived from the primary sequence of
795 the protein. Size exclusion chromatography (Superdex 200 Increase) was used to remove high
796 molecular weight impurities prior to measuring the activities of the fusion proteins in bioassays.
797

798 **Receptor subunit ECD direct binding and competition binding assays.**

799 ***Binding determinations by ELISA***

800 Binding was determined using a competition binding ELISA. Microtiter plates (Immulon 4HBX
801 flat bottom 96-well) were coated with 50 µL of 1 mg/mL human ECDs: IL-7Rα(aa 21-236)-
802 His_6, Sino Biological Cat# 10975-H08H; cynomolgus IL-7Rα(aa 21-235)-His_6, Sino Biological
803 Cat# 90332-C08H; human IL-2Rα(aa 23-254)-Fc, Acro Cat# ILG-H5256; cynomolgus IL-

804 2Rα(aa 23-254)-Fc, made in-house, in PBS overnight at 4°C. The wells were emptied and
805 blocked with 300 µL of PBS containing 1% BSA (Bovine Serum Albumin Fraction V, VWR
806 Cat# 97061-416) for 1 h at 25°C. Blocked plates were washed 3 times with 300 µL wash buffer
807 (PBS containing 0.05% Tween-20). C-terminal biotinylated versions of the IL-7R binding
808 peptideMDK1248 and the γc binding peptide, MDK1188 were each pre-complexed with
809 Neutravidin-HRP for at least 45 min prior to use in the assays (10 µM bn-peptide and 0.13
810 mg/mL NA-HRP in PBS). The test compounds were serially diluted in assay buffer at twice the
811 final desired concentration, 50 µL was added to the assay plate and incubated for 1 h at 4°C.
812 Without washing, 50 µL of pre-complexed biotinylated peptide NA-HRP tracer (at final
813 concentration approximately equal to EC_{75}) was added, and the plate returned to 4°C for 45 min.
814 Plates were washed with cold wash buffer, and bound tracer was detected using TMB One
815 Component HRP substrate and Stop Solution (Surmodics Cat# TMBW-1000-01 and LSTP-
816 0100-01). Absorbance at 450 nm was read using Agilent BioTek Synergy HTX Multimode
817 Reader.
818
819 ***Binding kinetics determination by biolayer interferometry***
820 Label-free measurement of the equilibrium dissociation constant (K_D) for peptide binding to IL-
821 7Rα and γc extracellular domains with peptides was done by biolayer interferometry (BLI,
822 Gator™ instrument; Gator Bio, Palo Alto, CA) with small/molecule/antibody/protein (SMAP)
823 biosensors. SMAP surface chemistry allows high-capacity immobilization of biotinylated targets
824 and the measurement of interactions of low molecular weight compounds. BLI experiments were
825 run in 96-well black microtiter plates (200 µL volume per well) at 30°C and a shaker speed of
826 1000 RPM. Biosensors were preloaded with biotinylated targets or biotin in BLI buffer (PBS

827 containing 0.02% BSA and 0.002% Tween-20). Biotinylated recombinant human receptor
828 extracellular domains (ECD) were purchased from Acro Biosystems IL-7Rα (aa 21-236)-Fc
829 huIgG1 receptor, Cat# IL7-H5258 and hexa-His tagged IL-2Rγ (aa 23-254), Cat# ILG-H85E8).
830 Biotin was purchased from Sigma Cat# B4501. Binding assays were performed as follows: (1)
831 biosensors were preloaded at a high density (7-10 nM) with biotinylated receptor ECDs or biotin
832 (saturating level); (2) 30 sec baseline; (3) 120 sec association for IL-7Rα, and 420 sec for IL-
833 2Rγ; (4) 180 sec for IL-7Rα and 660 sec dissociation for IL-2Rγ; (5) 30 sec baseline. A double-
834 reference procedure was used, wherein two biosensors were loaded with each biotinylated
835 receptor, and two biosensors were loaded with biotin. Receptor coated tips were exposed to
836 increasing peptide concentrations (2-fold dilutions) or no peptide. The second receptor coated tip
837 was iteratively exposed to assay buffer. The negative control tips, coated with biotin, were
838 iteratively exposed to the same peptide titration and buffer as was the receptor of interest. Raw
839 data was processed with the instrument data analysis software (v1.7.2). Double reference
840 subtracted data was processed with the recommended software options and subjected to a
841 Savitzky-Golay filter and fit to a 1:1 binding model (local for IL-7Rα and global for IL-2Rγ).
842 The curve fit was used to determine the association rate constants (k_a; units M^{-1} sec^{-1}) and the
843 dissociation rate constants (k_d; units sec^{-1}). Equilibrium dissociation constants (K_D; units
844 nanomolar (nM)) were calculated as a ratio of k_d/k_a.
845

846 **Preparation of cell lines, PBMCs, and isolated T-lymphocyte subsets.**

847 ***Construction and maintenance of cell lines responsive to individual γc cytokines or TSLP***

848 To construct cell lines responsive to each of the γc family cytokines, TF-1 cells were purchased
849 from American Type Culture Collection (ATCC Cat # CRL-2003) and cultured in RPMI 1640

850 supplemented with 4.5 g/L glucose, 10% FBS, 2 mM L-glutamine, 1mM sodium pyruvate, 10
851 mM HEPES, penicillin-streptomycin, and 2 ng/mL GM-CSF (TF-1 cells naturally express γc and
852 IL-4Rα). Transfections were performed with an Amaxa Nucleofector device: $2x10^6$ cells were
853 resuspended in 100 μL Nucleofector solution T (Lonza) and added to 2 μg of pcDNA3.1
854 expression vector encoding full-length IL-2Rβ, IL-7Rα, IL-9Rα, or IL-21Rα; and electroporation
855 was performed with Nucleofector program T-001 (for UniProt accession numbers see S2 Table).
856 Following electroporation, cells were immediately added to RPMI medium and allowed to
857 recover overnight. The next day Geneticin was added to the cultures to select for stable pools of
858 transfected cells. Following antibiotic selection, cells were transitioned from GM-CSF-
859 supplemented medium to medium supplemented with 40 ng/mL IL-2, 15 ng/mL IL-7, 10 ng/mL
860 IL-9, or 25 ng/mL IL-21, respectively.
861
862 To construct a TSLP-responsive cell line, the TF-1-7Rα cell line described above was
863 transfected with 2.0 μg pcDNA3.1 expression vector encoding full-length TSLPR (CFLR2, S2
864 Table), using the Amaxa Nucleofector device with Nucleofector program T-001. Following
865 transfection, the cells were immediately added to RPMI 1640 medium supplemented with 4.5
866 g/L glucose, 10% FBS, 2 mM L-glutamine, 1 mM sodium pyruvate, 10 mM HEPES, 100 IU/mL
867 penicillin, 100 μg/mL streptomycin, and 20 ng/mL IL-7 and allowed to recover overnight.
868 Hygromycin selection was used to establish a stable pool of cells expressing TSLPR. The cells
869 were cultured for 1-2 weeks in IL-7 supplemented medium and tested by flow cytometry for
870 TSLPR and IL-7Rα expression. The TF-1-7Rα/TSLPR positive pool was then bulk sorted to
871 enrich the high-expressing TSLPR population by Stanford Medicine Shared FACS Facility staff.
872 The sorted pool was cultured in TF-1 RPMI medium supplemented with 20 ng/mL IL-7.

873

874 ***Preparation of human PBMCs and lymphocyte subtypes.***

875 Human donor buffy coats were purchased from Stanford Blood Center, and PBMCs were
876 isolated by centrifugation in Lymphoprep™ density gradient medium (Stemcell Technologies
877 Cat# 07811). The plasma layer was discarded, the white mononuclear cell layer was decanted
878 and washed twice with cold PBS + 2% FBS, and cell count and viability were determined.
879 For preparation of lymphocyte subsets, naïve CD4+ T-cells were isolated via two-stage negative
880 selection with EasySep™ Human Naïve CD4+ T-Cell Isolation Kit II (Stemcell Technologies
881 Cat# 17555); and CD8+ T-cells were isolated by negative selection from PBMCs with Stem Cell
882 Technology Easy Sep CD8+ kit, or obtained freshly prepared from Stanford Blood Center.
883 Rested naïve CD4+ T-cells or CD8+ T-cells were prepared by overnight incubation at 37°C, 5%
884 CO_2 in CTS™ OpTmizer™ T-Cell Expansion SFM (ThermoFisher Scientific Cat# A1048501).

885

886 ## Cell-based assays

887 ***STAT phosphorylation assays***

888 Cells were deprived of growth factors by overnight incubation at 5×10^5 cells/mL in starvation
889 medium (RPMI 1640 + 4.5 g/L glucose + 0.2% FBS + 2 mM L-glutamine + 1 mM NaPyr + 10
890 mM HEPES + 0.5x penicillin-streptomycin with no cytokine supplement) in T75 flasks. For
891 assays, cells were plated in 96-well V-bottom plates at 2×10^5 cells/well. Three-fold serial
892 dilutions in starvation medium of the test compounds or cytokine were added to the cells and
893 incubated for 30 min at 37°C. Following incubation, cell extracts were prepared by adding a
894 mixture of 10x Cell Lysis Buffer (Cell Signaling Technology Cat# 9803) and 100x HALT
895 Phosphatase and Protease Inhibitor Cocktail (Thermo Fisher Cat# 78442) directly to the wells.

896 The plates were agitated at 25°C for 5 min to prepare cell extracts for immediate use or to be
897 stored at -80°C until assay. Detection of pSTAT5 was performed using a PathScan® Phospho-
898 Stat5 (pTyr694) Sandwich ELISA Kit (Cell Signaling Technology Cat# 7113). Detection of
899 pSTAT6 was performed using a PathScan® Phospho-Stat6 (pTyr641) Sandwich ELISA Kit
900 (Cell Signaling Technology Cat# 7275). Detection of pSTAT3 was performed using a
901 PathScan® Phospho-Stat3 (pTyr705) Sandwich ELISA Kit (Cell Signaling Technology Cat#
902 7300). Cell lysates were added to pre-coated ELISA wells and incubated at 4°C overnight.
903 Primary and secondary antibody incubations and wash steps were performed according to the
904 protocols supplied by the manufacturer. Assays were developed using TMB substrate
905 (Surmodics Cat# TMBW-1000-01) for 5-10 min at 25°C and the reaction was stopped using
906 STOP solution (Surmodics Cat# LSTP-1000-01).
907 To detect phopho-STAT5 in immune subsets of PBMCs by flow cytometry, frozen
908 human and cynomolgus macaques PBMCs (Stemcell Technologies, Cat# 70025.2 and iQ
909 Biosciences, Cat# IQB-MnPB102, respectively) from 5 different healthy donors were thawed
910 and rested overnight in T-cell media (CTS™ OpTmizer™ T-Cell Expansion SFM,
911 ThermoFisher Scientific Cat# A1048501) at 37ºC. Cells were stained with a viability dye for 30
912 min at 37ºC followed by surface marker antibodies for 30 min on ice (S3 Table), then treated
913 with serially diluted test compounds in the medium for 30 min. The cells were then washed,
914 fixed, permeabilized as instructed by the manufacturer, and stained with pSTAT5 and
915 intracellular antibodies for 50 min on ice. Antibody-stained cells were analyzed immediately by
916 flow cytometry using the Novocyte Advanteon instrument (Agilent), and the data were analyzed
917 using FlowJo software. Fluorescence minus one (FMO) controls were used to draw gates. For
918 measuring pSTAT5 in activated PBMCs, the overnight rested cells were incubated with

919 CD3/CD28 Dynabeads at 1 bead to 1 cell ratio for 3 days and then rested for 2 days in the fresh
920 medium without the Dynabeads before testing the compounds.
921
922 ***Proliferation of PBMC subpopulations***
923 Human PBMCs were isolated from buffy coats by density gradient centrifugation
924 (Lymphoprep®, Stemcell Technologies Cat# 07811) and cultured overnight in T-cell medium
925 (CTS OpTmizer®, ThermoFisher Cat# A1048501) at 3×10^6 cells/mL in T75 flasks. The
926 following day, cells were resuspended in fresh medium and split into activated and rested groups
927 upon plating. To activate cells, 96-well plates were pre-coated with 10 ng/mL anti-CD3 mAb at
928 4°C overnight (Purified NA/LE mouse anti-human CD3, BD Cat# 557052). Three-fold serial
929 dilutions of either IL-7 or a test compound were added to the cells and incubated for 4 days at
930 37°C. After treatment, cells were incubated in viability dye (Live/Dead® Fixable Aqua Cell
931 Stain Kit, ThermoFisher Cat# L34965) for 30 min at 37°C, then stained with surface marker
932 antibodies in PBS + 2% FBS for 30 min on ice. Cells were fixed and permeabilized with
933 Fixation/Permeabilization Buffer (eBioscience Foxp3/Transcription Staining Buffer Set,
934 ThermoFisher Cat# 00-5523-00) for 30 min on ice. Intracellular (Ki-67) staining was then
935 performed in Permeabilization Buffer for 30 min on ice, and the treated cells resuspended in PBS
936 + 2% FBS prior to flow cytometer analysis.
937
938 ***IL-7Rα (CD127) internalization assay***
939 CD8+ cells isolated by negative selection from PBMCs with Stem Cell Technology Easy Sep
940 CD8+ kit, or obtained freshly prepared from Stanford Blood Center, were rested overnight in
941 RPMI 1640 containing Pen/Strep, L-Glutamine and 20% FBS; then resuspended to 7.0 $\times10^6$

942 cells/mL. Surface IL-7R was preloaded by treating the cells with saturating concentrations of the
943 test and control compounds for 20 min on ice, then shifted to 37°C to allow internalization. At
944 various times samples were taken, and each time point was quenched by returning samples to
945 internalization-restrictive ice-cold conditions. Following collection of the timed incubations, the
946 cells were washed 2x with cold PBS + 2% FBS and stained with anti-CD127-Alexa Fluor® 488
947 (anti-IL-7Rα) (antibody clone 40131; R&D Systems Cat# FAB306G) for 30 min on ice,
948 protected from light, and fixed with 100 μL of 1.5% paraformaldehyde (16% stock diluted into
949 PBS). To determine levels of cell surface IL-7Rα, analysis was performed by flow cytometry to
950 determine median fluorescence intensity (MFI) of cells at each condition.
951 Negative controls consisted of a blank (no compound added); MDK1169, a peptide
952 agonist of another γc family receptor (which contains a γc binding domain similar to MDK1472
953 but lacking the IL-7Rα binding domain); and MDK-202, an Fc-fusion of MDK1169 (a construct
954 analogous to MDK-703, with the same IgG2 Fc domain fusion partner) [59]. A parallel assay
955 with all compounds held on ice for the duration of the time course was also performed. Flow data
956 was collected as MFI, and for display, data was normalized with blank value setting the upper
957 limit of 100% surface CD127, and the signal baseline (0%) estimated by adding an excess of
958 unlabeled antibody clone 40131 for 30 min on ice prior to staining with the labeled detection
959 antibody.
960
961 ***Analysis of effects of test compounds on activation of all gamma common family receptors,***
962 ***and the TSLP receptor***
963 TF-1-derived lines separately expressing each gamma common family private receptor were
964 starved overnight at $5x10^5$ cells/mL. The following day, the cells were counted and plated at

965 $2x10^6$ cells/well in 96-well plates. Dose response assays of pSTAT activation by the gamma
966 common cytokines IL-2, IL-4, IL-7, IL-9, IL-15, and IL-21 were performed with three-fold serial
967 dilutions of the cytokines added to the respective cytokine receptor-expressing TF-1 cells and
968 incubated for 30 min at 37°C to estimate EC_{75} levels. To assess inhibition of the activities of
969 these cytokines, the test compounds MDK1188, MDK1248, MDK1472, or MDK-703 were
970 serially diluted in starvation medium, and pre-incubated with the cells for 20 min at 37°C. Sub-
971 maximal levels (EC_{75}) of each cytokine were then added to the corresponding cells for 30 min at
972 37°C. Cell extracts were prepared and analyzed for pSTAT3, pSTAT5, or pSTAT6 accumulation
973 with Pathscan pSTAT ELISA kits as described above. Human IL-2, IL-4, IL-7, IL-9, IL-15, and
974 IL-21 were obtained from Peprotech (Cat#s 200-02, 200-04, 200-07, 200-09, 200-15, and 200-
975 21).

976 To evaluate the effect of MDK-703 on TSLP receptor-mediated signaling, pSTAT5
977 assays were run using the engineered IL-7Rα/TSLPR cell line. In each assay, the cells were
978 starved overnight at $5x10^5$ cells/mL, counted, and $1.8x10^5$ cells/well were plated in 96-well
979 plates. These cells respond to both IL-7 and to TSLP with the production of pSTAT5. To
980 separately measure TSLP receptor activation in the presence of the IL-7R agonist MDK-703, the
981 interaction of MDK-703 with γc was blocked by the inclusion of 20uM of a high affinity
982 competitive inhibitor of the interaction, MDK2058. IL-7 and TSLP receptor activation assays
983 were run 30 min at 37˚C and pSTAT5 accumulation was detected with PathScan Phospho-Stat5
984 (Tyr694) Sandwich ELISA Kit, Cell Signaling Technology Cat#7113 to quantitate the response.
985 Absorbance at 450 nm was read using Agilent BioTek Synergy HTX Multimode Reader (Figs 2
986 A and 2B). In the same assay, the dose response of pSTAT5 activation by TSLP was measured

987 with or without preincubation with the gamma common chain blocker MDK2058, +/- MDK-703
988 at EC_{95} (600 nM final concentration), for 4 min at 4°C (Fig 4H).
989
990 ***PBMC proliferation***
991 Frozen human PBMCs from 5 healthy donors (Stemcell Technologies, Cat# 70025.2, Lot
992 numbers 2108409012, 2109407009, 210680104C, 210680801C, 211280501C, 220781802C)
993 were thawed and rested overnight at 37°C, 5% CO_2 in CTS™ OpTmizer™ T-Cell Expansion
994 SFM (ThermoFisher Scientific Cat# A1048501). Four million cells in 2 mL media were cultured
995 in the plate coated with or without 10 ng/mL of CD3 antibody (Clone SP34-2) and in the
996 presence or absence of 100 nM MDK-703 or 1 nM IL-7. Fresh media containing MDK-703 and
997 IL-7 were provided every 4-5 days. At indicated time points, cell aliquots were taken, and cell
998 surface staining was performed using antibodies shown in S3 Table followed by viability dye
999 staining. For Ki-67 and FoxP3 staining, surfaced stained cells were fixed and permeabilized
1000 according to the manufacturer's instructions and analyzed immediately using the Novocyte
1001 Advanteon instrument (Agilent). The data were analyzed using FlowJo software. Fluorescence
1002 Minus One (FMO) controls were used to draw gates. Percentages of Ki-67+ cell populations
1003 were expressed as average ± SEM. Memory T-cells are as follows: Tn
1004 (CD45RA+CCR7+CD28+CD95-), Tscm (CD45RA+CCR7+CD28+CD95+), Tem (CD45RA-
1005 CCR7-), Tcm (CD45RA-CCR7+), and Temra (CD45RA+CCR7-). To count cells per well, at
1006 each assay time point 50 μL of the cells were taken from each well and incubated with 200 μL of
1007 the viability dye solution. The NovoCyte Advanteon flow cytometer was set to analyze precisely
1008 50 μL (12.5 μL original culture volume), which allowed the calculation of the absolute live cell

1009 counts. Because the culture volumes change over time due to splitting and removal, dilution
1010 factors were considered when calculating the total number of cells.

1011 ***Pharmacodynamic study with humanized NSG mice***

1012 The PD study was performed at Crown Biosciences (San Diego, CA). Ten HIS-NSG mice
1013 (NSG™ NOD.Cg-Prkdcscid Il2rgtm1Wjl, Stock No. 005557) engrafted with CD34+ cells from
1014 2 donors (The Jackson Laboratory, Bar Harbor, ME) were treated intravenously once with 1
1015 mg/kg of MDK-703 or a human Fc control. Blood samples were collected via submandibular
1016 bleeding on day 7, and terminal blood samples were collected via cardiac puncture. Red blood
1017 cells were removed using RBC Lysis Buffer (BioLegend Cat#-420302). Spleens were harvested
1018 on day 12 and processed to single-cell suspensions using the Gentle MACS, program
1019 m_spleen_04. Cell aggregates were removed by passing through a 70 μm pore filter, and red
1020 blood cells were lysed. Splenocytes were incubated with TruStain FcX before antibody staining
1021 as described above. Antibody-stained cells were acquired by using BD LSRFortessa X-20 flow
1022 cytometer and analyzed with Kaluza software.

1023 ***Single dose pharmacokinetic and pharmacodynamic studies of MDK-703 in NHP***

1024 NHP studies were conducted at Envol Biomedical (Naples, FL). For the PD study, 3 female
1025 cynomolgus macaques were dosed once subcutaneously at 0.3 mg/kg MDK-703, and blood
1026 samples were collected at days 1(pre-dose), 2, 3, 4, 6, 8, 12, 18, 24, 30, 36, and 42 days and
1027 analyzed by complete blood count and flow cytometry. For the PK study, 3 female macaques per
1028 group were dosed once with 1 mg/kg MDK-703 via intravenous bolus, subcutaneous, or
1029 intramuscular injection. Blood samples were collected at Pre-Dose (day 1), 0.5, 1 h, 2 h, 4 h, 8 h,
1030 24 h, 48 h, 72 h, 96 h, 120 h, 144 h, 168 h, 192 h, and 216 h post-dose into serum separator vials
1031 and processed for serum (30 min at room temperature followed by centrifugation at 4°C, 3000 x

1032 g for 5 min). The serum was transferred to a polypropylene tube and stored at -80°C until
1033 analysis. A standard sandwich ELISA using a three-fold dilution of serum samples was
1034 performed to quantify the amount of MDK-703. For plasma samples from subcutaneously
1035 injected animals, a biotinylated rat polyclonal antibody against human Fc was used as a capture
1036 antibody and anti-human IgG Fc-HRP (GenScript Cat# A01854-200) as a detection antibody.
1037 For plasma samples from the intravenous or intramuscular injection, biotinylated mouse anti-
1038 human IgG2 Fc (Southern Biotech Cat# 9070-08) was used as a capture antibody and rabbit
1039 polyclonal antibody raised against IL-7Rγ peptide agonist followed by a mouse anti-rabbit IgG
1040 Fc HRP (Genscript Cat# A01856-200) as a detection antibody. The quantity of MDK-703 in
1041 each serum sample was calculated with a standard curve of the test compound diluted in the
1042 control cynomolgus monkey serum. Individual animal serum MDK-703 concentration versus
1043 time data was imported into Phoenix WinNonlin v8.3 (Certara, Princeton, NJ) for analysis. All
1044 values that were less than the lower limit of quantitation (LLOQ) of the assay were treated as
1045 missing for the PK analyses. The individual animal concentration versus time data was analyzed
1046 using a noncompartmental model with extravascular administration. Nominal dose and sample
1047 collection times were used in estimating the PK parameters.

1048 # Acknowledgments

1049 The authors would like to acknowledge Julie Crider, PhD, for medical editing contributions.
1050

References

1051

1052 1. Puel A, Ziegler SF, Buckley RH, Leonard WJ. Defective IL7R expression in T(-)B(+)NK(+)
1053 severe combined immunodeficiency. Nat Genet. 1998;20(4):394-7. doi: 10.1038/3877.
1054 2. Cunningham-Rundles C, Ponda PP. Molecular defects in T- and B-cell primary
1055 immunodeficiency diseases. Nature Rev Immunol. 2005;5(11):880-92. doi: 10.1038/nri1713.
1056 3. Kim GY, Hong C, Park JH. Seeing is believing: illuminating the source of in vivo interleukin-
1057 7. Immune Netw. 2011;11(1):1-10. doi: 10.4110/in.2011.11.1.1.
1058 4. Ariel A, Hershkoviz R, Cahalon L, Williams DE, Akiyama SK, Yamada KM, et al. Induction
1059 of T cell adhesion to extracellular matrix or endothelial cell ligands by soluble or matrix-bound
1060 interleukin-7. Eur J Immunol. 1997;27(10):2562-70. doi: 10.1002/eji.1830271015.
1061 5. Winer H, Rodrigues GOL, Hixon JA, Aiello FB, Hsu TC, Wachter BT, et al. IL-7:
1062 Comprehensive review. Cytokine. 2022;160:156049. doi: 10.1016/j.cyto.2022.156049.
1063 6. Link A, Vogt TK, Favre S, Britschgi MR, Acha-Orbea H, Hinz B, et al. Fibroblastic reticular
1064 cells in lymph nodes regulate the homeostasis of naive T cells. Nat Immunol. 2007;8(11):1255-
1065 65. doi: 10.1038/ni1513.
1066 7. Sasson SC, Zaunders JJ, Kelleher AD. The IL-7/IL-7 receptor axis: understanding its central
1067 role in T-cell homeostasis and the challenges facing its utilization as a novel therapy. Curr Drug
1068 Targets. 2006;7(12):1571-82. doi: 10.2174/138945006779025365.
1069 8. Fry TJ, Mackall CL. Interleukin-7: master regulator of peripheral T-cell homeostasis? Trends
1070 Immunol. 2001;22(10):564-71. doi: 10.1016/s1471-4906(01)02028-2.
1071 9. Park JH, Yu Q, Erman B, Appelbaum JS, Montoya-Durango D, Grimes HL, et al.
1072 Suppression of IL7Ralpha transcription by IL-7 and other prosurvival cytokines: a novel
1073 mechanism for maximizing IL-7-dependent T cell survival. Immunity. 2004;21(2):289-302. doi:
1074 10.1016/j.immuni.2004.07.016.
1075 10. Fry TJ, Mackall CL. The many faces of IL-7: from lymphopoiesis to peripheral T cell
1076 maintenance. J Immunol. 2005;174(11):6571-6. doi: 10.4049/jimmunol.174.11.6571.
1077 11. Mazzucchelli R, Durum SK. Interleukin-7 receptor expression: intelligent design. Nature
1078 Rev Immunol. 2007;7(2):144-54. doi: 10.1038/nri2023.
1079 12. ElKassar N, Gress RE. An overview of IL-7 biology and its use in immunotherapy. J
1080 Immunotoxicol. 2010;7(1):1-7. doi: 10.3109/15476910903453296.
1081 13. Kim R, Barve M, Mamdani H, Johnson M, Lee BH, Ferrando-Martinez S, et al. 404. Initial
1082 biomarker and clinical data of a phase 2a study of NT-I7, a long-acting interleukin-7, plus

1083 pembrolizumab: cohort of subjects with checkpoint inhibitor-naïve advanced MSS-colorectal
1084 cancer. J Immunother Cancer. 2021;9(Suppl 2):A435-A. doi: 10.1136/jitc-2021-SITC2021.404.
1085 14. Gastman B, Fling S, Ansstas G, Funchain P, W. SA, Friedlander PA, et al. A phase 1b/2a
1086 study of safety and efficacy of NT-I7 in combination with anti-PD-L1 (atezolizumab) in patients
1087 with anti-PD-1/PD-L1 naïve or relapsed/refractory (R/R) high-risk skin cancers: The phase 1b
1088 report. J Clin Oncol. 2022;40(16_suppl):9561-. doi: 10.1200/JCO.2022.40.16_suppl.9561.
1089 15. Gattinoni L, Speiser DE, Lichterfeld M, Bonini C. T memory stem cells in health and
1090 disease. Nat Med. 2017;23(1):18-27. doi: 10.1038/nm.4241.
1091 16. Mackall CL, Fry TJ, Gress RE. Harnessing the biology of IL-7 for therapeutic application.
1092 Nat Rev Immunol. 2011;11(5):330-42. doi: 10.1038/nri2970.
1093 17. Barata JT, Durum SK, Seddon B. Flip the coin: IL-7 and IL-7R in health and disease. Nat
1094 Immunol. 2019;20(12):1584-93. doi: 10.1038/s41590-019-0479-x.
1095 18. Gao J, Zhao L, Wan YY, Zhu B. Mechanism of action of IL-7 and its potential applications
1096 and limitations in cancer immunotherapy. Int J Mol Sci. 2015;16(5):10267-80. doi:
1097 10.3390/ijms160510267.
1098 19. Morre M, Beq S. Interleukin-7 and immune reconstitution in cancer patients: a new
1099 paradigm for dramatically increasing overall survival. Target Oncol. 2012;7(1):55-68. doi:
1100 10.1007/s11523-012-0210-4.
1101 20. Sheikh V, Porter BO, DerSimonian R, Kovacs SB, Thompson WL, Perez-Diez A, et al.
1102 Administration of interleukin-7 increases CD4 T cells in idiopathic CD4 lymphocytopenia.
1103 Blood. 2016;127(8):977-88. doi: 10.1182/blood-2015-05-645077.
1104 21. Tredan O, Menetrier-Caux C, Ray-Coquard I, Garin G, Cropet C, Verronese E, et al.
1105 ELYPSE-7: a randomized placebo-controlled phase IIa trial with CYT107 exploring the
1106 restoration of CD4+ lymphocyte count in lymphopenic metastatic breast cancer patients. Ann
1107 Oncol. 2015;26(7):1353-62. doi: 10.1093/annonc/mdv173.
1108 22. Thiebaut R, Jarne A, Routy JP, Sereti I, Fischl M, Ive P, et al. Repeated Cycles of
1109 Recombinant Human Interleukin 7 in HIV-Infected Patients With Low CD4 T-Cell
1110 Reconstitution on Antiretroviral Therapy: Results of 2 Phase II Multicenter Studies. Clin Infect
1111 Dis. 2016;62(9):1178-85. doi: 10.1093/cid/ciw065.

1112 23. Merchant MS, Bernstein D, Amoako M, Baird K, Fleisher TA, Morre M, et al. Adjuvant
1113 Immunotherapy to Improve Outcome in High-Risk Pediatric Sarcomas. Clin Cancer Res.
1114 2016;22(13):3182-91. doi: 10.1158/1078-0432.CCR-15-2550.
1115 24. Francois B, Jeannet R, Daix T, Walton AH, Shotwell MS, Unsinger J, et al. Interleukin-7
1116 restores lymphocytes in septic shock: the IRIS-7 randomized clinical trial. JCI Insight.
1117 2018;3(5). doi: 10.1172/jci.insight.98960.
1118 25. Lee SW, Choi D, Heo M, Shin EC, Park SH, Kim SJ, et al. hIL-7-hyFc, A Long-Acting IL-
1119 7, Increased Absolute Lymphocyte Count in Healthy Subjects. Clin Transl Sci. 2020;13(6):1161-
1120 9. doi: 10.1111/cts.12800.
1121 26. Miskin DP, Chalkias SG, Dang X, Bord E, Batson S, Koralnik IJ. Interleukin-7 treatment of
1122 PML in a patient with idiopathic lymphocytopenia. Neurol Neuroimmunol Neuroinflamm.
1123 2016;3(2):e213. doi: 10.1212/NXI.0000000000000213.
1124 27. Naing A, Kim R, Barve M, Johnson M, Lee BH, Ferrando-Martinez S, et al. 408.
1125 Preliminary biomarker and clinical ata of a phase 2a study of NT-I7, a long-acting interleukin-7,
1126 plus pembrolizumab: cohort of subjects with checkpoint inhibitor-naïve advanced pancreatic
1127 cancer. J Immunother Cancer. 2021;9(Suppl 2):A439-A. doi: 10.1136/jitc-2021-SITC2021.408.
1128 28. Campian JL, Luo J, Avvaru C, Katumba R, Kim AH, Dunn GP, et al. A phase I/II study to
1129 evaluate the safety and efficacy of a novel long-acting interleukin-7, NT-I7, for patients with
1130 newly diagnosed high-grade gliomas after chemoradiotherapy: The interim result of the phase I
1131 data. J Clin Oncol. 2021;39(15_suppl):2040-. doi: 10.1200/JCO.2021.39.15_suppl.2040.
1132 29. Kim JH, Kim YM, Choi D, Jo SB, Park HW, Hong SW, et al. Hybrid Fc-fused interleukin-7
1133 induces an inflamed tumor microenvironment and improves the efficacy of cancer
1134 immunotherapy. Clin Transl Immunol. 2020;9(9):e1168. doi: 10.1002/cti2.1168.
1135 30. Kim R, Mamdani H, Barve M, Johnson M, Sahin I, Kopetz S, et al. P-54 Phase 2a study of
1136 NT-I7, a long-acting interleukin-7, plus pembrolizumab: Cohort of subjects with checkpoint
1137 inhibitor-naïve advanced MSS-colorectal cancer. Ann Oncol. 2022;33:S266. doi:
1138 10.1016/j.annonc.2022.04.144.
1139 31. Naing A, Mamdani H, Barve M, Johnson M, Wolff R, Kim D, et al. P-48. Phase 2a study of
1140 NT-I7, a long-acting interleukin-7, plus pembrolizumab: Cohort of subjects with checkpoint
1141 inhibitor-naïve advanced pancreatic cancer. Ann Oncol. 2022;33:S263-S4. doi:
1142 10.1016/j.annonc.2022.04.138.

1143 32. Naing A, Mamdani H, Barve MA, Johnson ML, Morgensztern D, Olszanski AJ, et al.
1144 Efficacy and safety of NT-I7, long-acting interleukin-7, plus pembrolizumab in patients with
1145 advanced solid tumors: Results from the phase 2a study. J Clin Oncol. 2022;40(16_suppl):2514-.
1146 doi: 10.1200/JCO.2022.40.16_suppl.2514.
1147 33. Sohn J, Kim GM, Lee KS, Kim S-B, Kim JH, Ahn HK, et al. Phase 1b/2 study of GX-I7
1148 plus pembrolizumab in patients with refractory or recurrent (R/R) metastatic triple-negative
1149 breast cancer (mTNBC): The KEYNOTE-899 Study. J Clin Oncol. 2022;40:1081.
1150 34. Wrighton NC, Farrell FX, Chang R, Kashyap AK, Barbone FP, Mulcahy LS, et al. Small
1151 peptides as potent mimetics of the protein hormone erythropoietin. Science.
1152 1996;273(5274):458-64. doi: 10.1126/science.273.5274.458.
1153 35. Cwirla SE, Balasubramanian P, Duffin DJ, Wagstrom CR, Gates CM, Singer SC, et al.
1154 Peptide agonist of the thrombopoietin receptor as potent as the natural cytokine. Science.
1155 1997;276(5319):1696-9. doi: 10.1126/science.276.5319.1696.
1156 36. Moise L, Gutierrez AH, Bailey-Kellogg C, Terry F, Leng Q, Abdel Hady KM, et al. The
1157 two-faced T cell epitope: examining the host-microbe interface with JanusMatrix. Hum Vaccin
1158 Immunother. 2013;9(7):1577-86. doi: 10.4161/hv.24615.
1159 37. Moise L, Gutierrez A, Kibria F, Martin R, Tassone R, Liu R, et al. iVAX: An integrated
1160 toolkit for the selection and optimization of antigens and the design of epitope-driven vaccines.
1161 Hum Vaccin Immunother. 2015;11(9):2312-21. doi: 10.1080/21645515.2015.1061159.
1162 38. Leonard WJ, Lin JX, O'Shea JJ. The gamma(c) Family of Cytokines: Basic Biology to
1163 Therapeutic Ramifications. Immunity. 2019;50(4):832-50. doi: 10.1016/j.immuni.2019.03.028.
1164 39. Lin JX, Leonard WJ. The common cytokine receptor gamma chain family of cytokines.
1165 Cold Spring Harb Perspect Biol. 2018;10(9). doi: 10.1101/cshperspect.a028449.
1166 40. Ebina-Shibuya R, Leonard WJ. Role of thymic stromal lymphopoietin in allergy and
1167 beyond. Nature Rev Immunol. 2023;23(1):24-37. doi: 10.1038/s41577-022-00735-y.
1168 41. Rosenberg SA, Sportès C, Ahmadzadeh M, Fry TJ, Ngo LT, Schwarz SL, et al. IL-7
1169 administration to humans leads to expansion of CD8+ and CD4+ cells but a relative decrease of
1170 CD4+ T-regulatory cells. J Immunother. 2006;29(3):313-9. doi:
1171 10.1097/01.cji.0000210386.55951.c2.

1172 42. Liu W, Putnam AL, Xu-Yu Z, Szot GL, Lee MR, Zhu S, et al. CD127 expression inversely
1173 correlates with FoxP3 and suppressive function of human CD4+ T reg cells. J Exp Med.
1174 2006;203(7):1701-11. doi: 10.1084/jem.20060772.
1175 43. Bradley LM, Haynes L, Swain SL. IL-7: maintaining T-cell memory and achieving
1176 homeostasis. Trends Immunol. 2005;26(3):172-6. doi: 10.1016/j.it.2005.01.004.
1177 44. Tan JT, Ernst B, Kieper WC, LeRoy E, Sprent J, Surh CD. Interleukin (IL)-15 and IL-7
1178 jointly regulate homeostatic proliferation of memory phenotype CD8+ cells but are not required
1179 for memory phenotype CD4+ cells. J Exp Med. 2002;195(12):1523-32. doi:
1180 10.1084/jem.20020066.
1181 45. Sprent J, Surh CD. Normal T cell homeostasis: the conversion of naive cells into memory-
1182 phenotype cells. Nat Immunol. 2011;12(6):478-84. doi: 10.1038/ni.2018.
1183 46. Tang AL, Teijaro JR, Njau MN, Chandran SS, Azimzadeh A, Nadler SG, et al. CTLA4
1184 expression is an indicator and regulator of steady-state CD4+ FoxP3+ T cell homeostasis. J
1185 Immunol. 2008;181(3):1806-13. doi: 10.4049/jimmunol.181.3.1806.
1186 47. Faller EM, Ghazawi FM, Cavar M, MacPherson PA. IL-7 induces clathrin-mediated
1187 endocytosis of CD127 and subsequent degradation by the proteasome in primary human CD8 T
1188 cells. Immunol Cell Biol. 2016;94(2):196-207. doi: 10.1038/icb.2015.80.
1189 48. Henriques CM, Rino J, Nibbs RJ, Graham GJ, Barata JT. IL-7 induces rapid clathrin-
1190 mediated internalization and JAK3-dependent degradation of IL-7Ralpha in T cells. Blood.
1191 2010;115(16):3269-77. doi: 10.1182/blood-2009-10-246876.
1192 49. Beq S, Rozlan S, Gautier D, Parker R, Mersseman V, Schilte C, et al. Injection of
1193 glycosylated recombinant simian IL-7 provokes rapid and massive T-cell homing in rhesus
1194 macaques. Blood. 2009;114(4):816-25. doi: 10.1182/blood-2008-11-191288.
1195 50. Chen D, Tang TX, Deng H, Yang XP, Tang ZH. Interleukin-7 biology and its effects on
1196 immune cells: mediator of generation, differentiation, survival, and homeostasis. Front Immunol.
1197 2021;12:747324. doi: 10.3389/fimmu.2021.747324.
1198 51. Daix T, Mathonnet A, Brakenridge S, Dequin PF, Mira JP, Berbille F, et al. Intravenously
1199 administered interleukin-7 to reverse lymphopenia in patients with septic shock: a double-blind,
1200 randomized, placebo-controlled trial. Ann Intensive Care. 2023;13(1):17. doi: 10.1186/s13613-
1201 023-01109-w.

1202 52. Lim JY, Kim NA, Lim DG, Eun C-y, Choi D, Jeong SH. Biophysical stability of hyFc
1203 fusion protein with regards to buffers and various excipients. Int J Biol Macromol. 2016;86:622-
1204 9. doi: https://doi.org/10.1016/j.ijbiomac.2016.02.006.
1205 53. Friend R, Baxter B, Park IA, Cwirla S, Barrett R. 625. A phase 1 single ascending dose
1206 study evaluating the safety, tolerability, and pharmacodynamic effects of MDK-703, an IL-7
1207 mimetic with extended half-life. J Immunother Cancer. 2022;10(Suppl 2):A657-A. doi:
1208 10.1136/jitc-2022-SITC2022.0625.
1209 54. Heninger AK, Theil A, Wilhelm C, Petzold C, Huebel N, Kretschmer K, et al. IL-7
1210 abrogates suppressive activity of human CD4+CD25+FOXP3+ regulatory T cells and allows
1211 expansion of alloreactive and autoreactive T cells. J Immunol. 2012;189(12):5649-58. doi:
1212 10.4049/jimmunol.1201286.
1213 55. Bernett MJ, Varma R, Bonzon C, Rashid R, Bogaert L, Liu K, et al. Abstract 5565: Potency-
1214 reduced IL15/IL15Rα heterodimeric Fc-fusions display enhanced in vivo activity through
1215 increased exposure. Cancer Res. 2018;78(13_Supplement):5565-. doi: 10.1158/1538-
1216 7445.Am2018-5565.
1217 56. Li L, Li Q, Yan ZX, Sheng LS, Fu D, Xu P, et al. Transgenic expression of IL-7 regulates
1218 CAR-T cell metabolism and enhances in vivo persistence against tumor cells. Sci Rep.
1219 2022;12(1):12506. doi: 10.1038/s41598-022-16616-2.
1220 57. Li Y, Wu D, Yang X, Zhou S. Immunotherapeutic Potential of T Memory Stem Cells. Front
1221 Oncol. 2021;11:723888. doi: 10.3389/fonc.2021.723888.
1222 58. Locke FL, Rossi JM, Neelapu SS, Jacobson CA, Miklos DB, Ghobadi A, et al. Tumor
1223 burden, inflammation, and product attributes determine outcomes of axicabtagene ciloleucel in
1224 large B-cell lymphoma. Blood Adv. 2020;4(19):4898-911. doi:
1225 10.1182/bloodadvances.2020002394.
1226 59. Dower WJ, Bakker AV, Cwirla SE, Williams BM, Joshi P, Pongtornpipat P, et al. Peptidyl
1227 IL-2/15Rβγc-restricted agonists, highly-attenuated and linked to anti-PD-1 antibodies to achieve
1228 selectivity and amplified potency in stimulating PD-1high lymphocytes. Society for
1229 Immunotherapy of Cancer (SITC) Nov 10-14, 2021; Washington, DC2021.
1230

1231

1232 # Supporting Information

1233 **S1 Fig. Plasma stability of MDK 1472 *in vitro.*** 10 mM MDK1472 or control peptide YGGFL
1234 incubated in duplicate in human or cynomolgus plasma at 37°C. At indicated time points,
1235 compounds were isolated from the plasma and the quantity of intact peptides measured by
1236 LC/MS/MS (Study performed by Quintara Discovery, Hayward, CA).

1237 **S2 Fig. Flow cytometry gating scheme for STAT5 and Ki-67 determinations in major**
1238 **lymphocyte populations of human PBMCs. (A) pSTAT5 assay. (B) Ki-67 assay.**

1239 **S3 Fig. Flow cytometry study of IL-7Rα internalization +/- exposure to test compounds.**
1240 Primary MFI data (A) plotted time course, (B) histograms, (C) gating scheme. (D) Evaluation of
1241 interference of IL-7 and IL-7Rα agonist test compounds, and irrelevant test compounds with
1242 detection of cell surface IL-7Rα on cell surface by labelled anti-CD127 Ab clone #40131. All
1243 test compounds are loaded on the cells on ice for 35 min, stained, and analyzed by flow (as
1244 described in detail in Methods).

1245 **S4 Fig. Flow cytometry gating scheme for analysis of T-memory cell Ki-67 expression and**
1246 **expansion of cell numbers following *in vitro* exposure of human PBMC to test compounds.**

1247 **S5 Fig. Proliferation of major lymphocyte subpopulations in humanized mice treated with**
1248 **test compounds.** (A) Day 7 cell counts in blood. (B) Day 12 Ki-67 in blood. (C) Day 7 memory
1249 T-cells Ki-67 in blood. (D) Day 12 Ki-67 in spleen**.**

1250 **S6 Fig. HIS mouse flow cytometry sample gating information.** (A) TBNK Ki-67+. (B) Tn
1251 and Tmem TCF1+.

1252 **S1 Table. Test compound potency.**

1253 **S2 Table. UniProt accession numbers.**

1254 **S3 Table. Labeled antibody reagents for flow cytometry studies.**

1255

A. Peptides

MDK1248 (IL-7Rα binding peptide) GWGIPWCTLDPGSLQCAWLGKHGG

MDK1188 (γc binding peptide) GGVVCQDWEGVELCWQGG

MDK1472 (IL-7R agonist peptide) GWGIPWCTLDPGSLQCAWLGKHGGGGSGGVVCQDWEGVELCWQGG

10 20 30 40

B. MDK1472

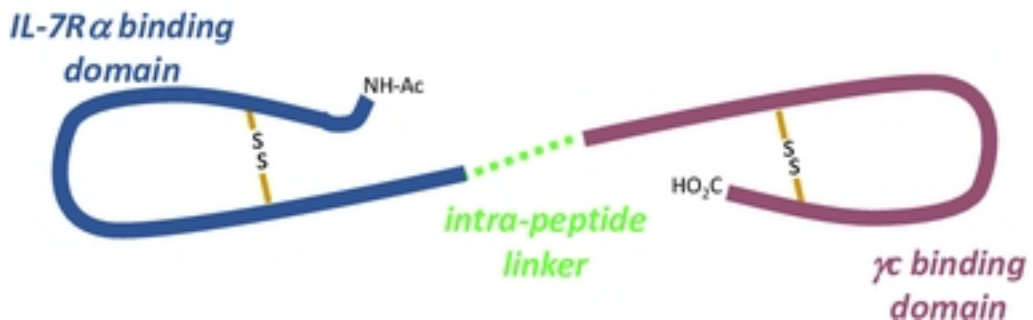

C. MDK-703

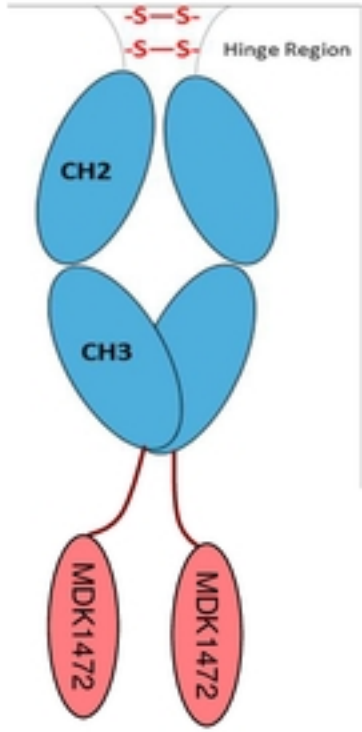

A

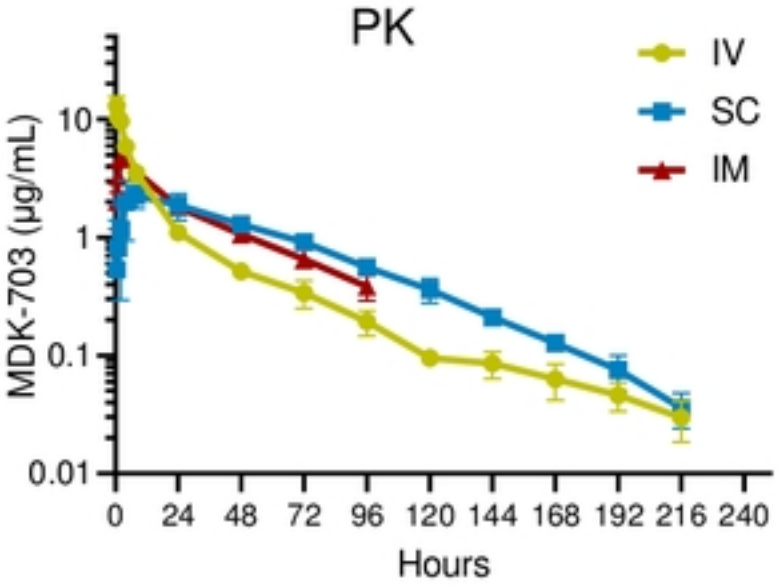
PK
IV
SC
IM
MDK-703 (µg/mL)
10
1
0.1
0.01
0
24
48
72
96
120
144
168
192
216
240
Hours

B

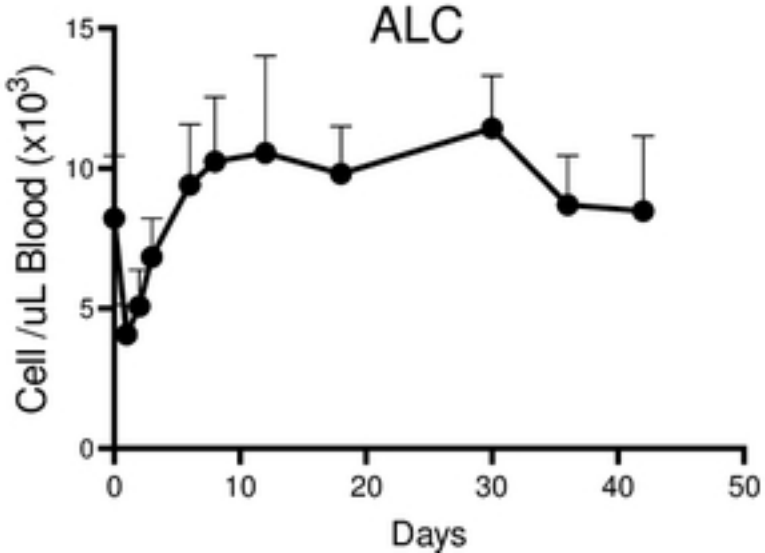
ALC
Cell /uL Blood (x10^3)
15
10
5
0
0
10
20
30
40
50
Days

C

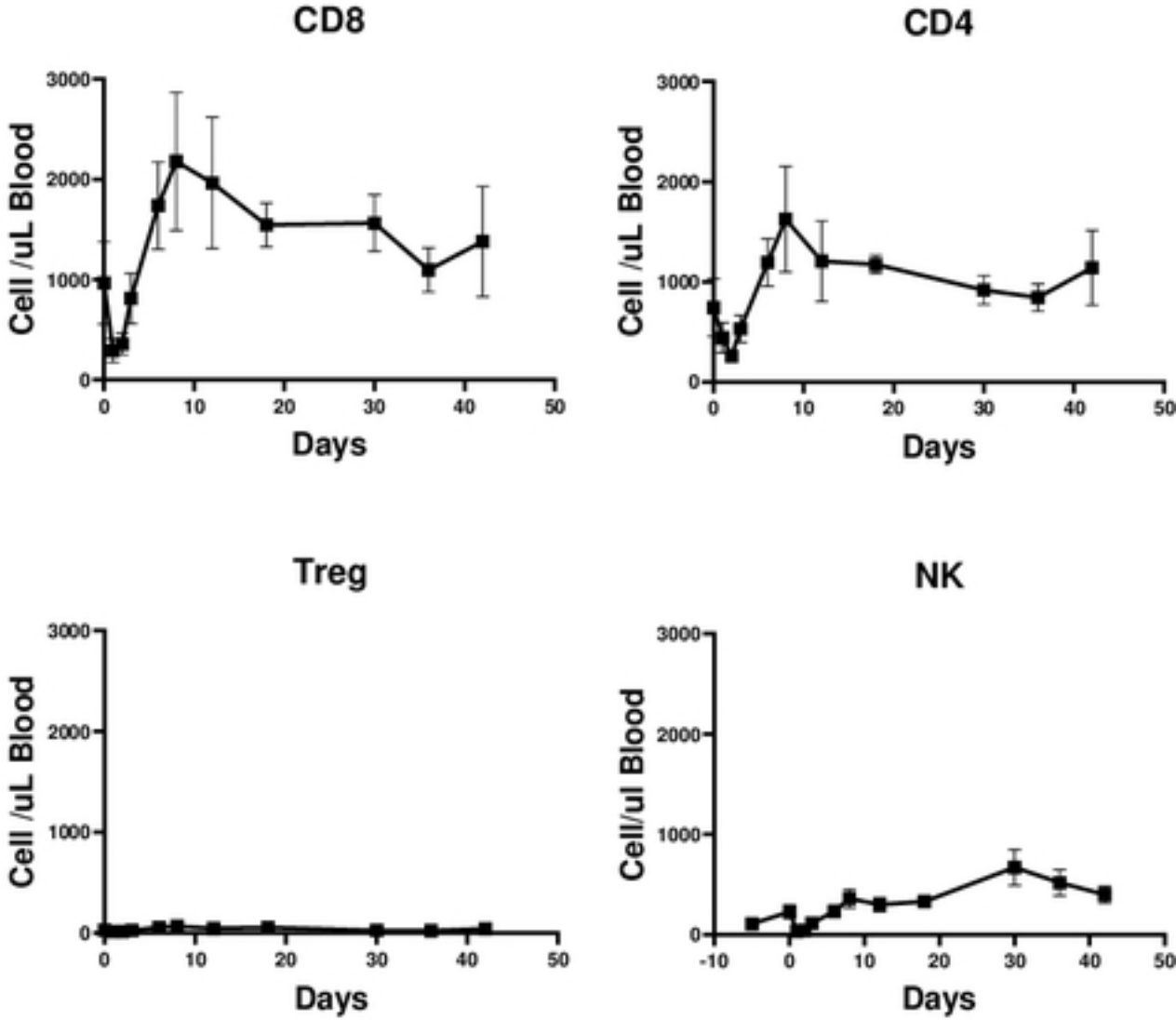
CD8
CD4
Treg
NK
Cell /uL Blood
Cell/ul Blood
3000
2000
1000
0
-10
0
10
20
30
40
50
Days

A

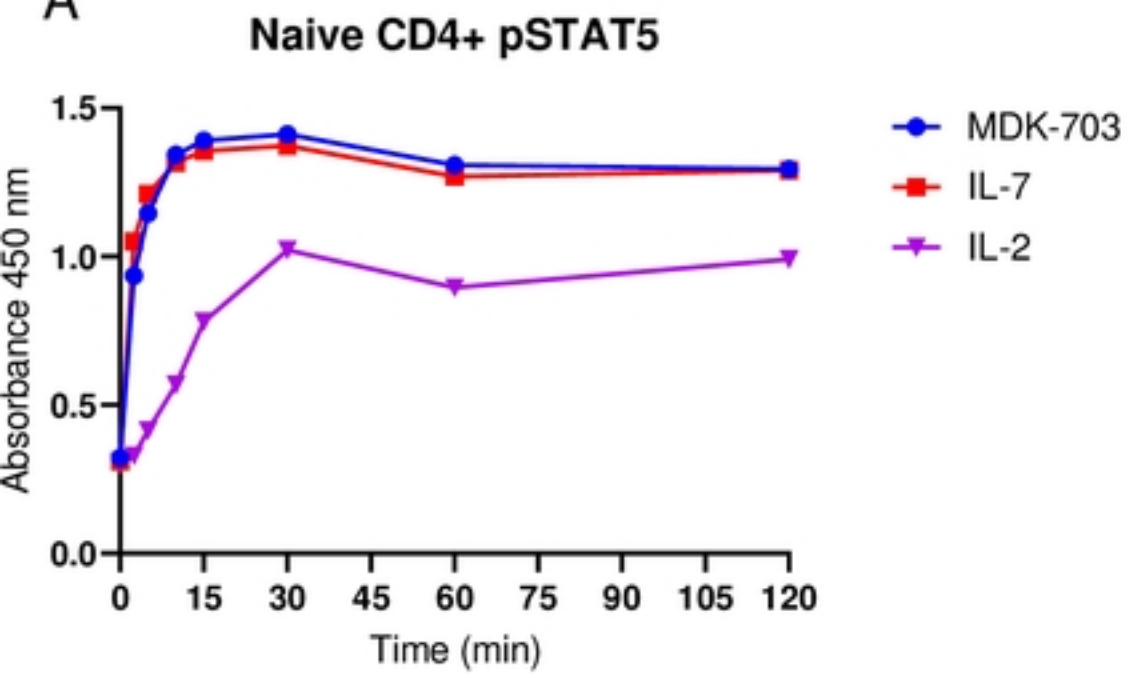

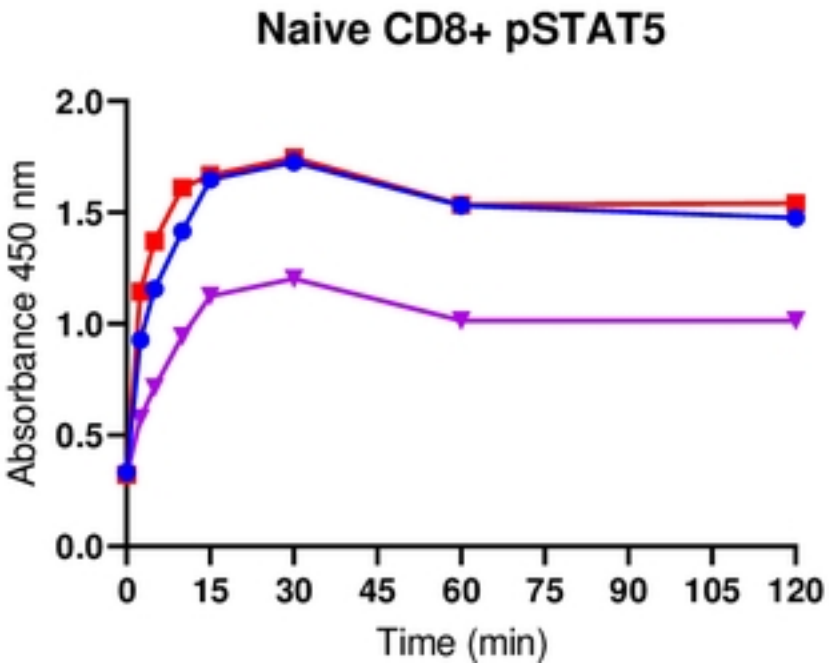

B

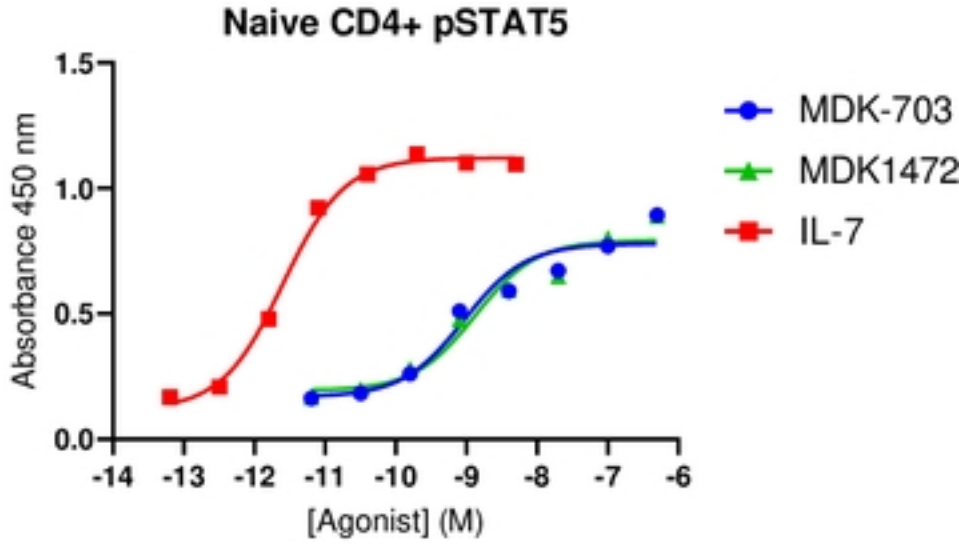

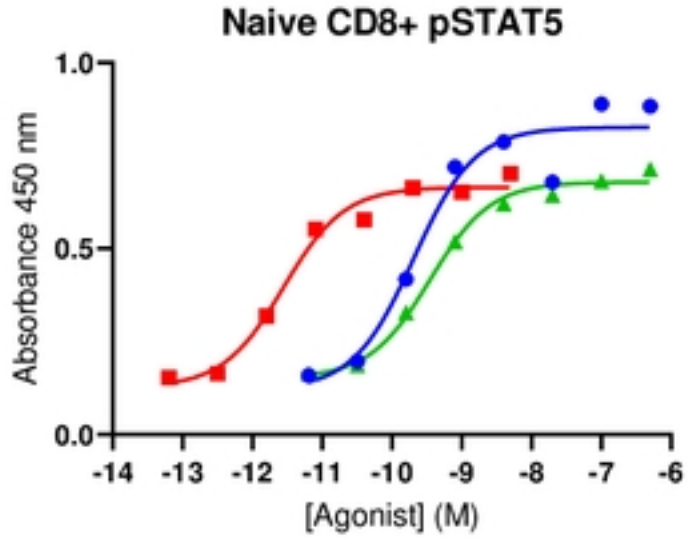

	EC_{50} (pM)		
Cell population	MDK-703	MDK1472	IL-7
CD4+	920	1,300	2.5
CD8+	201	350	2.8

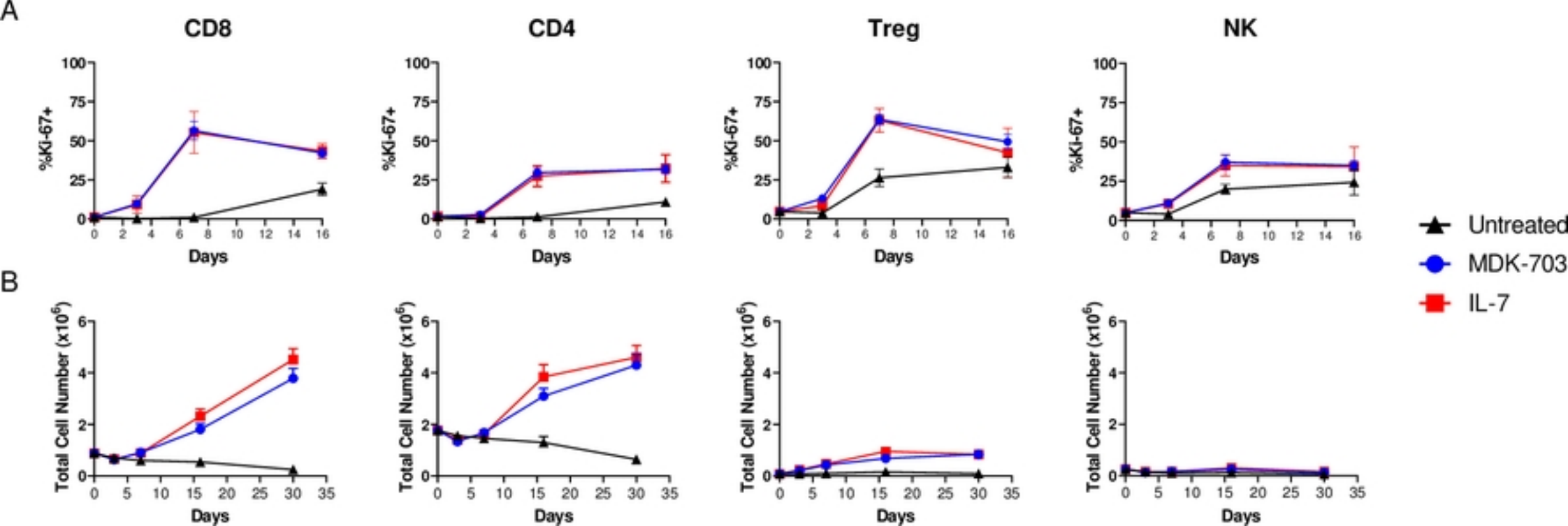
A
CD8
CD4
Treg
NK
%Ki-67+
Days
B
Total Cell Number (x10^6)
Days
Untreated
MDK-703
IL-7

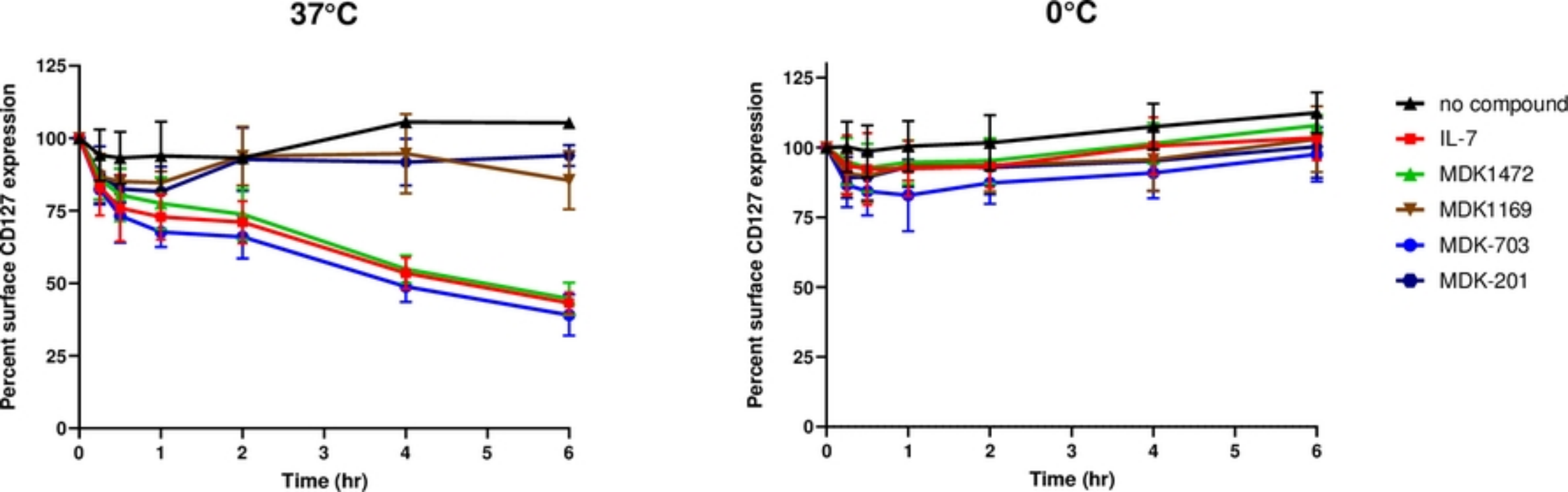
37°C
0°C
Percent surface CD127 expression
125
100
75
50
25
0
0
1
2
3
4
5
6
Time (hr)
no compound
IL-7
MDK1472
MDK1169
MDK-703
MDK-201

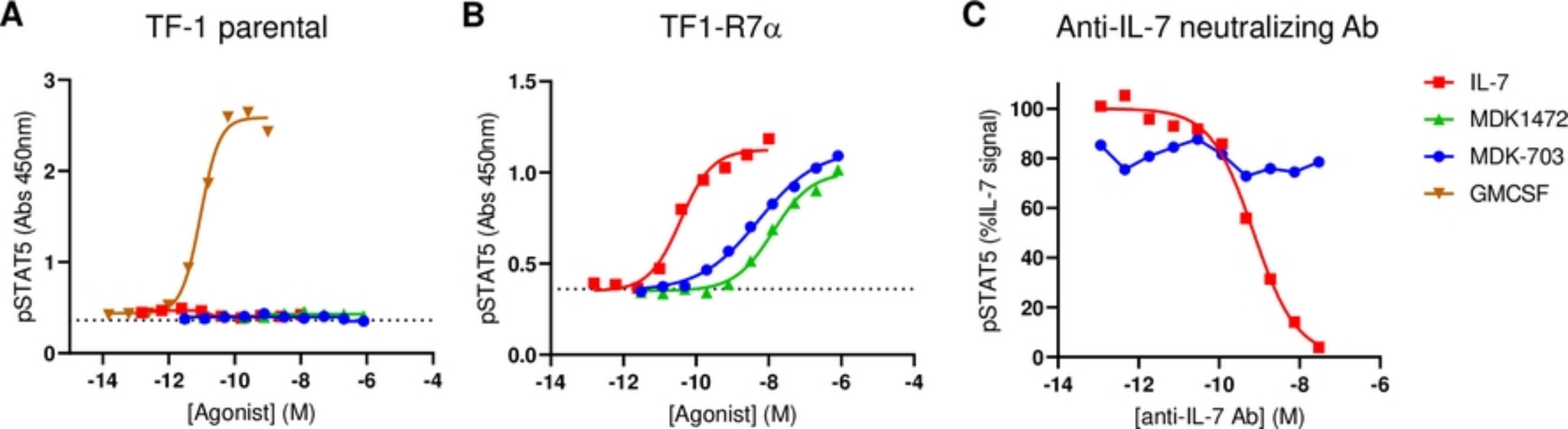
A
TF-1 parental
pSTAT5 (Abs 450nm)
[Agonist] (M)
B
TF1-R7α
pSTAT5 (Abs 450nm)
[Agonist] (M)
C
Anti-IL-7 neutralizing Ab
pSTAT5 (%IL-7 signal)
[anti-IL-7 Ab] (M)
IL-7
MDK1472
MDK-703
GMCSF

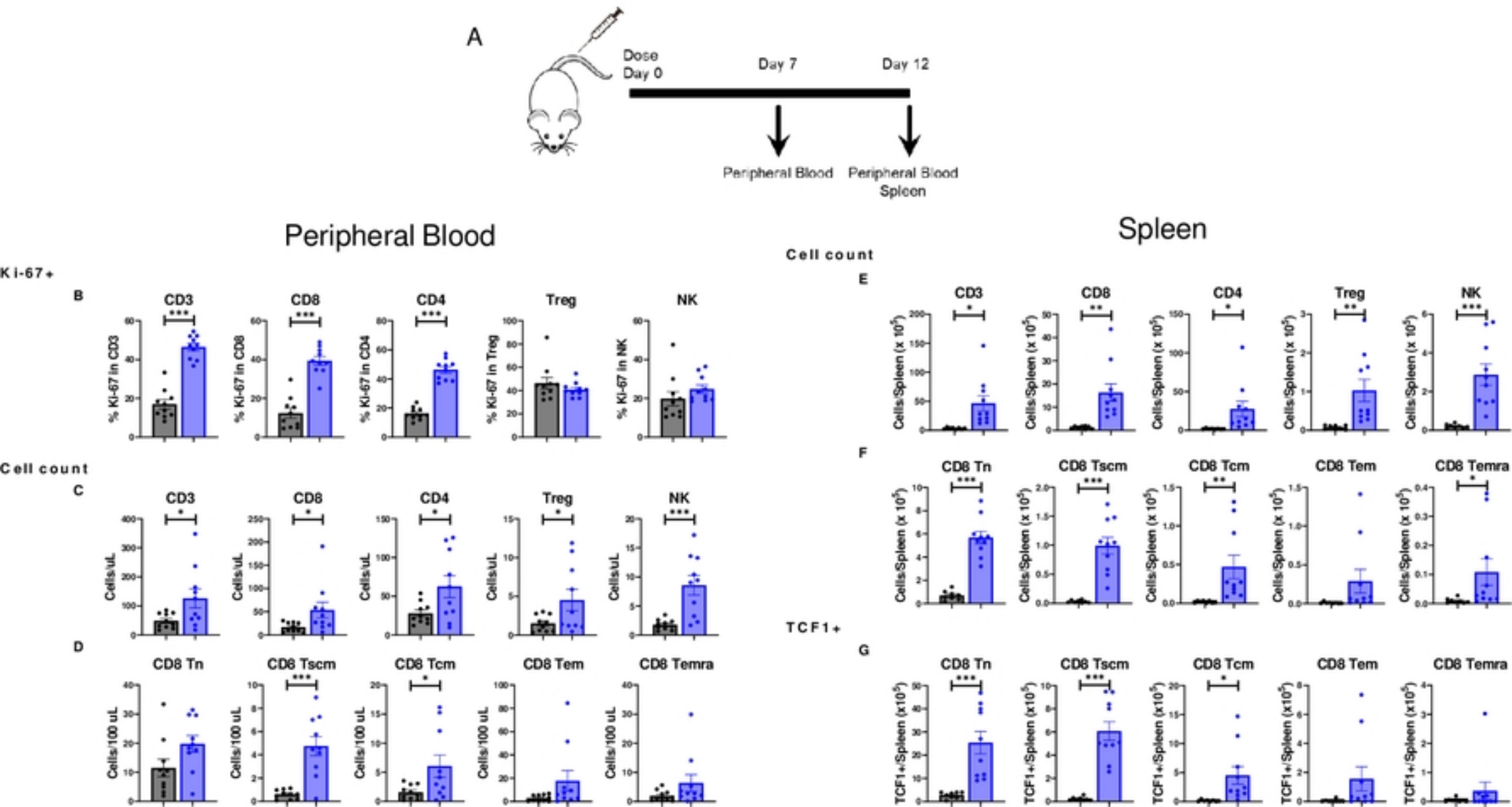
A
Dose
Day 0
Day 7
Day 12
Peripheral Blood
Peripheral Blood
Spleen
Peripheral Blood
Spleen
Ki-67+
B
CD3
CD8
CD4
Treg
NK
% Ki-67 in CD3
% Ki-67 in CD8
% Ki-67 in CD4
% Ki-67 in Treg
% Ki-67 in NK
Cell count
C
Cells/uL
D
CD8 Tn
CD8 Tscm
CD8 Tcm
CD8 Tem
CD8 Temra
Cells/100 uL
Cell count
E
Cells/Spleen (x 10^5)
F
TCF1+
G
TCF1+/Spleen (x10^5)

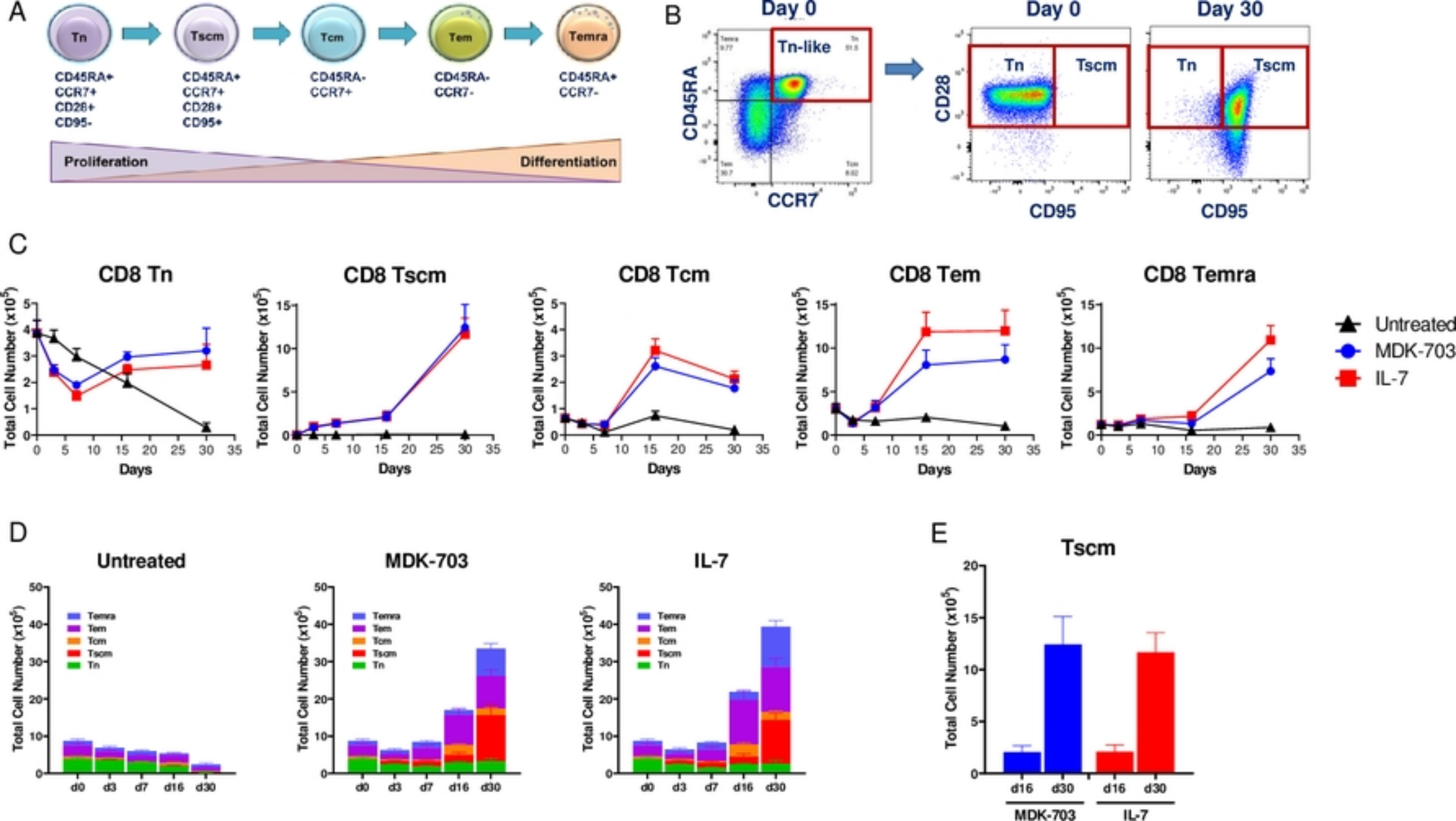
A
Tn
Tscm
Tcm
Tem
Temra
CD45RA+ CCR7+ CD28+ CD95-
CD45RA+ CCR7+ CD28+ CD95+
CD45RA- CCR7+
CD45RA- CCR7-
CD45RA+ CCR7-
Proliferation
Differentiation
B
Day 0
Day 0
Day 30
Tn-like
CD45RA
CCR7
CD28
CD95
Tn
Tscm
C
CD8 Tn
CD8 Tscm
CD8 Tcm
CD8 Tem
CD8 Temra
Total Cell Number (x10^5)
Days
Untreated
MDK-703
IL-7
D
Untreated
MDK-703
IL-7
Temra
Tem
Tcm
Tscm
Tn
d0
d3
d7
d16
d30
E
Tscm
MDK-703
IL-7

A human PBMCs, rested

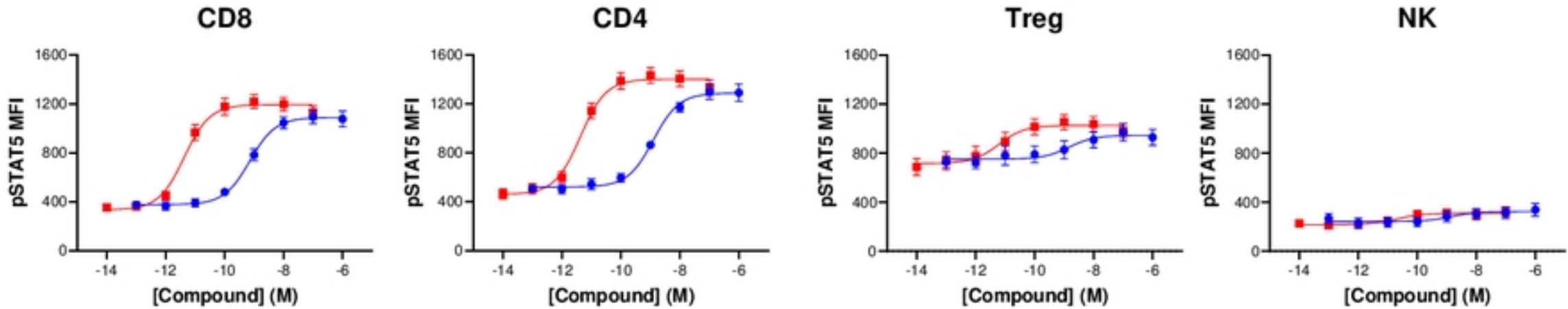

B human PBMCs, CD3/CD28 activated

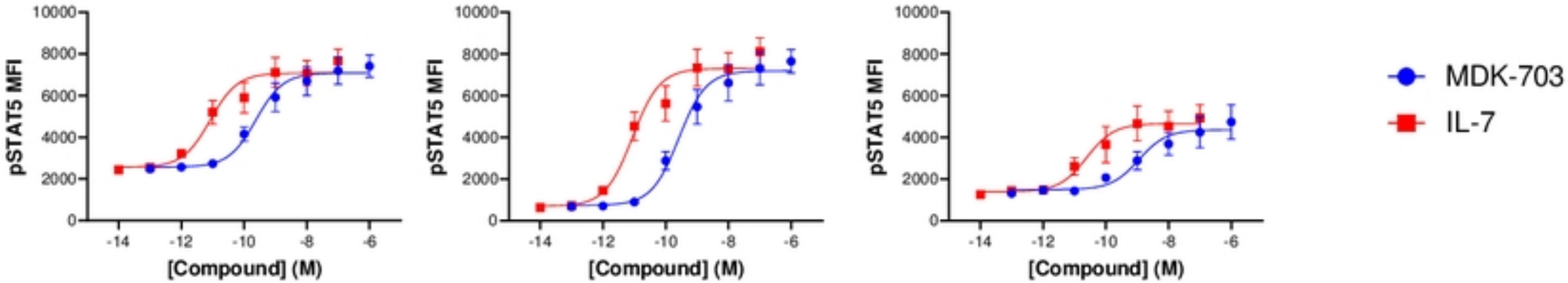

C cyno PBMCs, rested

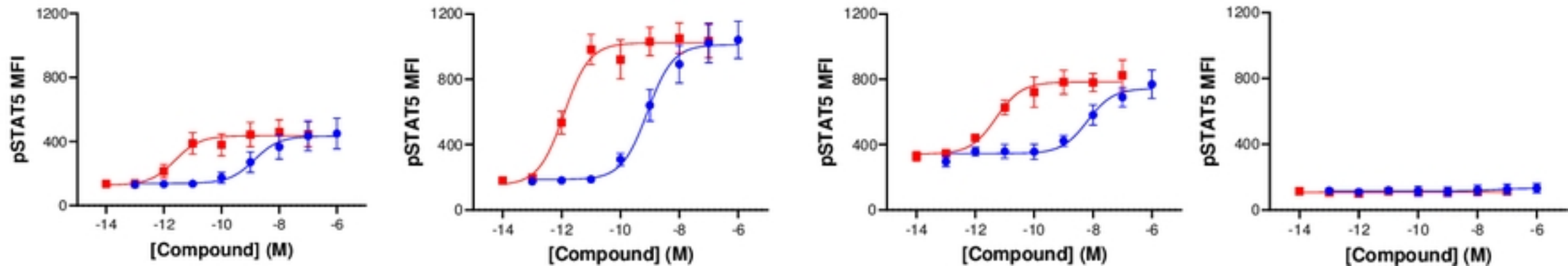

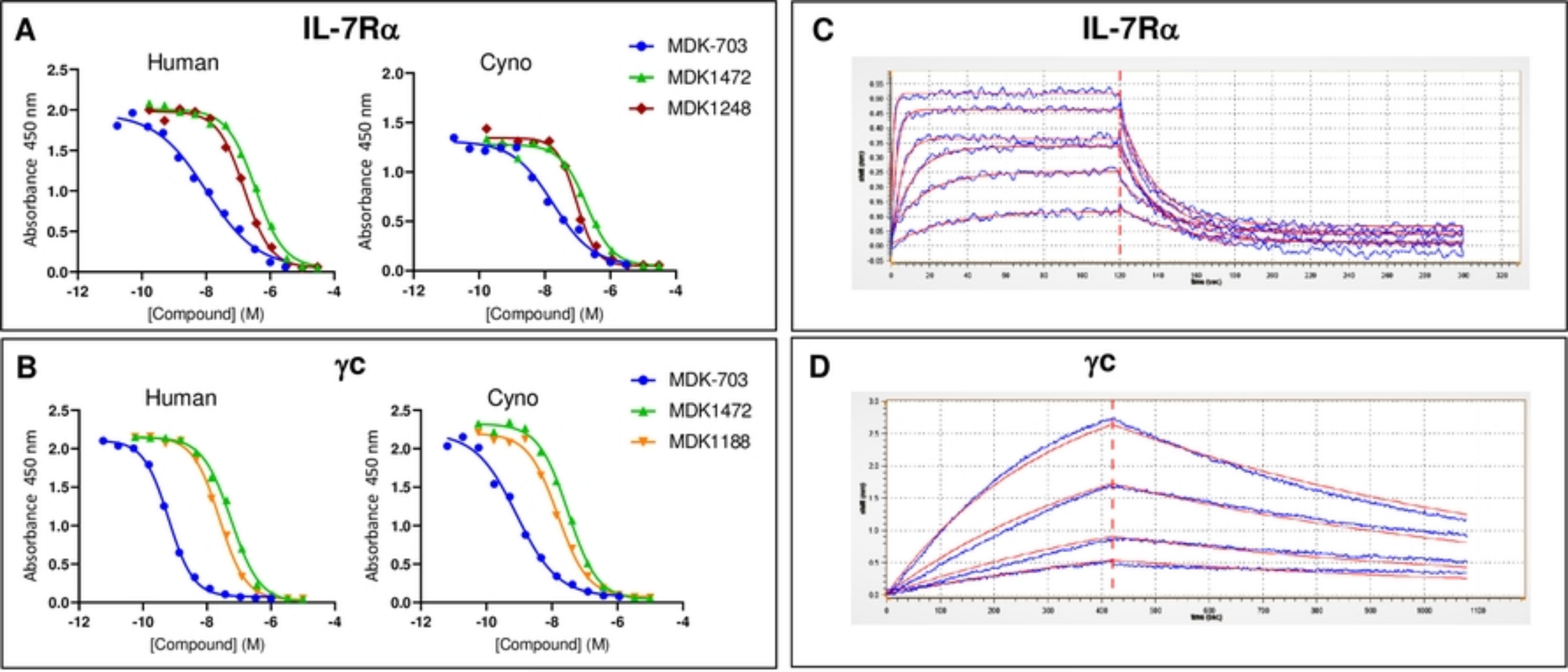

	Competition ELISA (IC_{50} nM)				BLI (KD nM)	
	IL-7Rα		γc		IL-7Rα	γc
Peptide	Human	Cyno	Human	Cyno	Human	Human
MDK1248	150	92	n.d.	n.d.	n.d.	n.d.
MDK1188	n.d.	n.d.	24	15	n.d.	n.d.
MDK1472	340	190	57	31	302	16
MDK-703	10	18	0.63	0.83	n.d.	n.d.

A

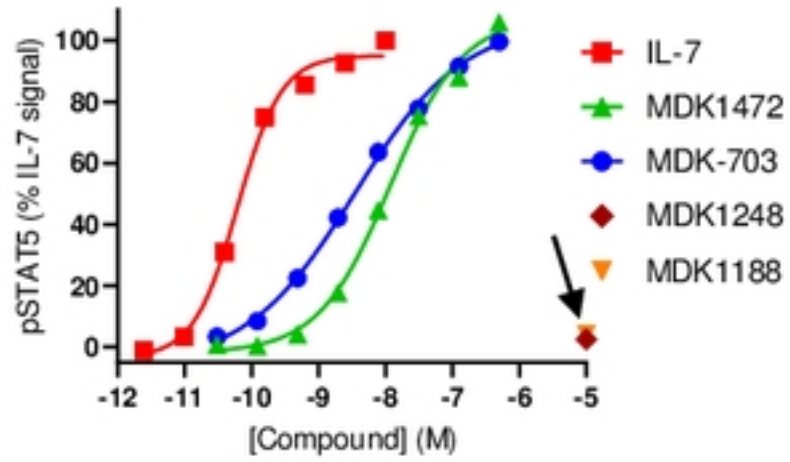

Compound	EC_{50} (nM)
IL-7	0.06
MDK1472	18
MDK-703	3.5

B

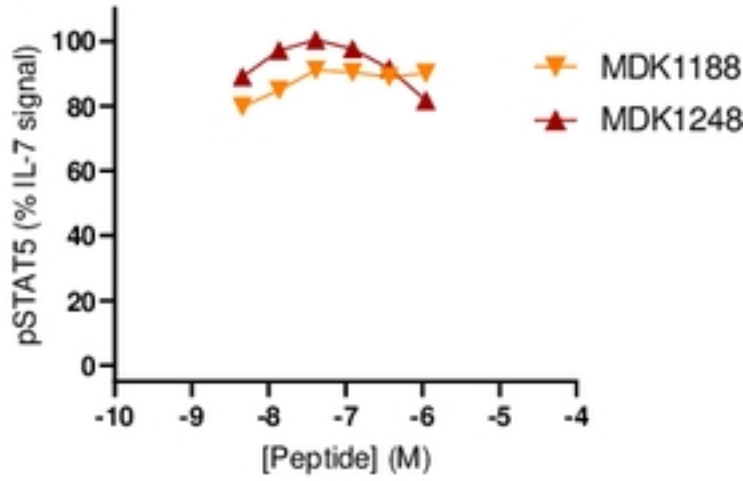

C

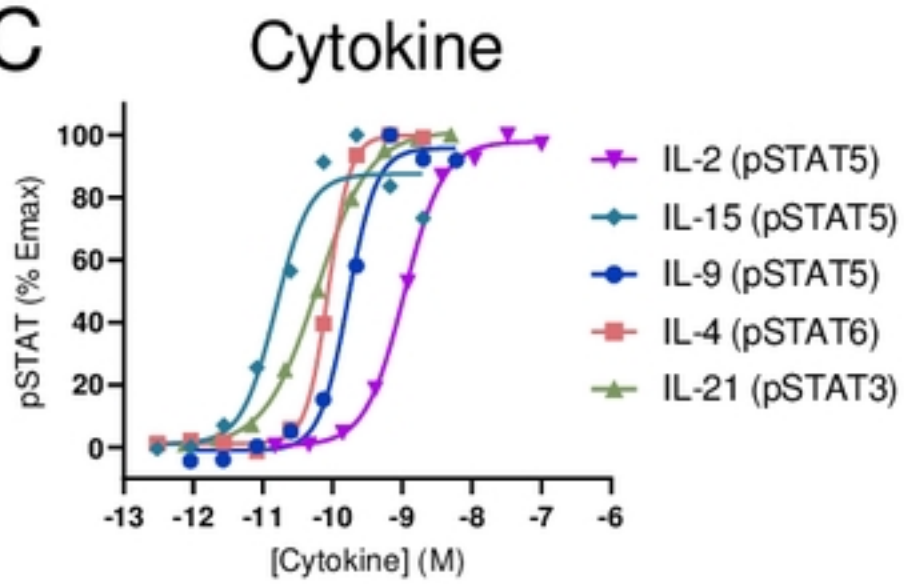

Cytokine	EC_{50} (pM)
IL-2	1100
IL-15	11
IL-9	170
IL-4	87
IL-21	60

D

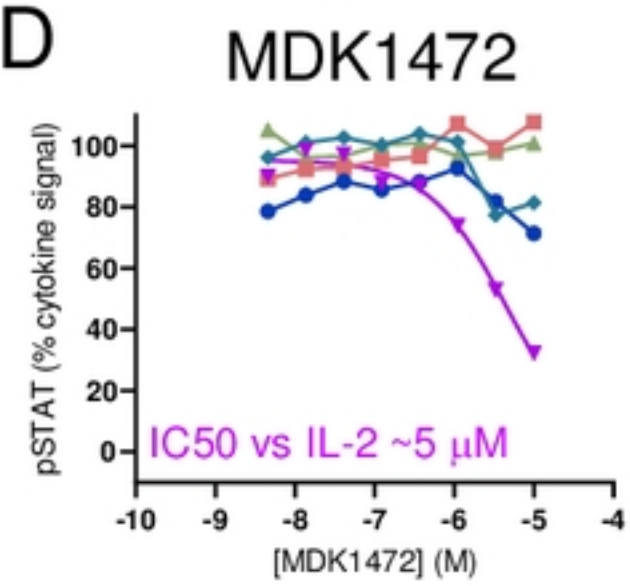

E

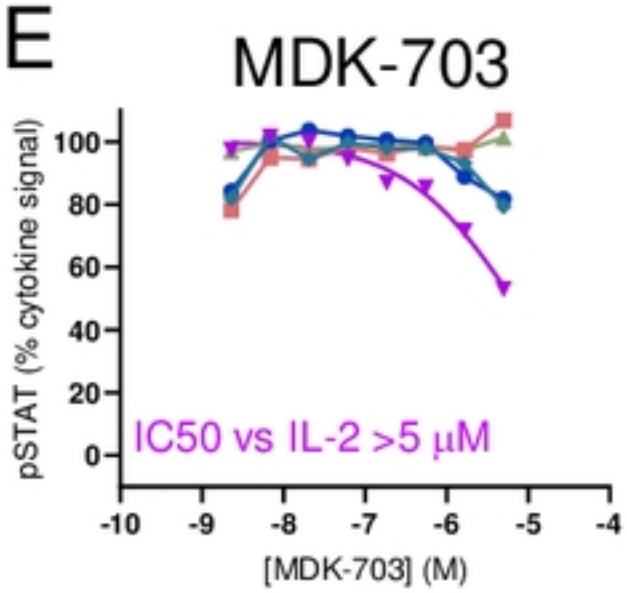

F

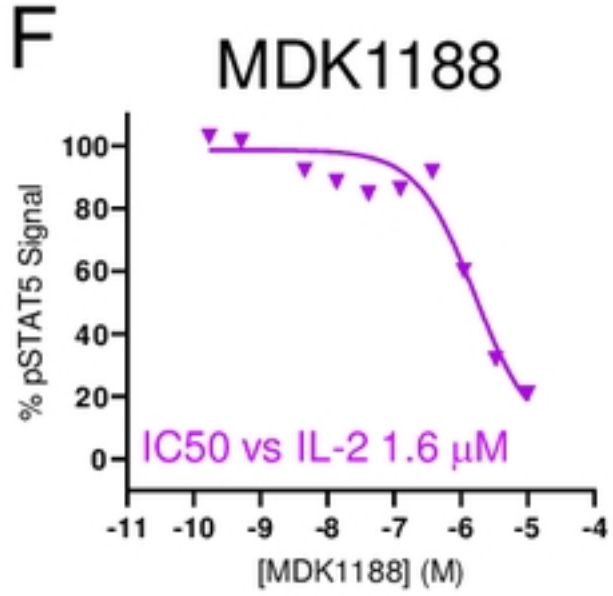

G

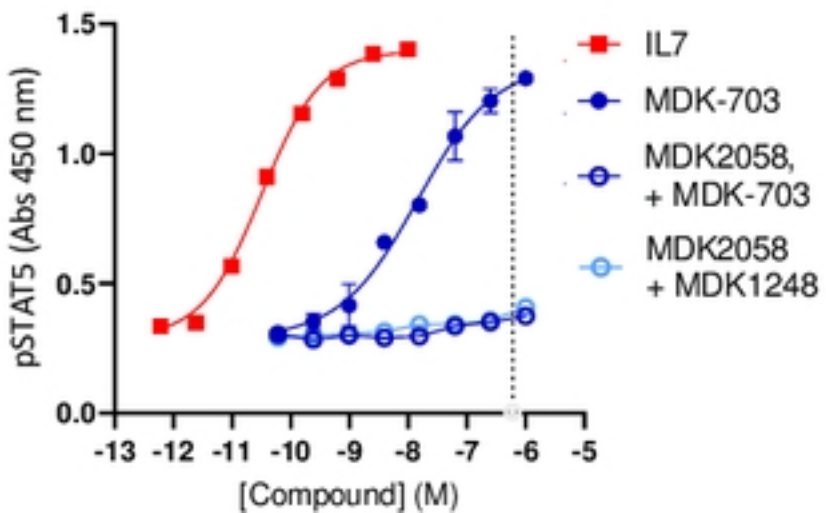

H

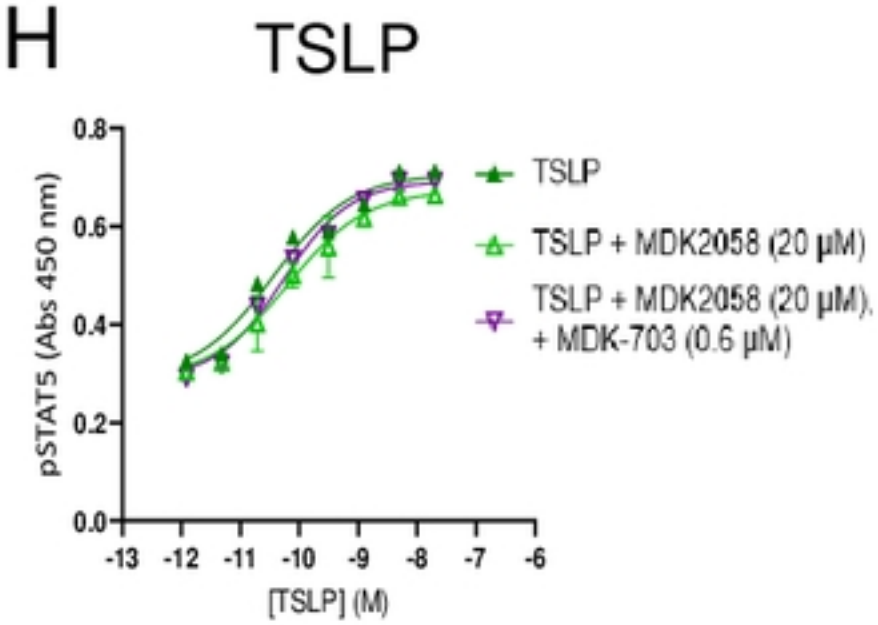

Agonist	EC_{50} (nM)
IL-7	0.03
MDK-703	14
TSLP	0.04
TSLP + MDK2058	0.06
TSLP + MDK2058, + MDK-703	0.05